

**An-Najah National University  
Faculty of Graduate Studies**

**The Magnetization of The (GaAs) Double  
Quantum Dots in a Magnetic Field**

**By  
Eshtiaq "Mohammed Yasir" Hijaz**

**Supervisor  
Prof. Dr. Mohammad Elsaid**

**Co-supervisor  
Dr. Musa Elhasan**

**This Thesis is Submitted in Partial Fulfillment of the  
Requirements for the Degree of Master of Physics, Faculty of  
Graduate Studies, An-Najah National University, Nablus,  
Palestine.**

**2016**

# The Magnetization of The (GaAs) Double Quantum Dots in a Magnetic Field

By

**Eshtiaq "Mohammed Yasir" Hijaz**

This thesis was defended successfully on 24/5/2016 and approved by:

**Defense committee members**

- Prof. Mohammed .K Elsaid /Supervisor
- Dr. Musa Elhasan /Co-Supervisor
- Dr. Marwan El-Kawni /External Examiner
- Dr. Khalid Ilawi /Internal Examiner

**Signature**

M. Khalid

M. Elhasan

El-Kawni

Khalid Ilawi

## Dedication

To my kind parents, who are impossible to be thanked adequately for everything they have done for me and my future and who learn me to be ambitious person. They always support me to get the best degrees. They are really the best model for perfect parents and they are the main cause of success in my life. God bless them.

To my beloved husband (*Loay*), who shares me all moments and help me to overcome difficulties to continue moving forward. He also provides me with encouragement, motivation and support to achieve my ambitions successfully.

To my lovely brothers (*Qusai, Mahmoud, Amr, Yazan & Zaid*), who always encourage me and give me a powerful support. They are always present to help and motivate me.

To my cute baby (*Omar*).

## **Acknowledgments**

All thanks to Allah, who give me with health, patience and knowledge to complete my thesis.

I would like to express my sincere thanks to my advisor and instructor Prof. Mohammed Elsaid for his guidance, assistance, supervision and contribution of valuable suggestions. And I would like to thank Dr. Musa Elhasan for his efforts and time. In addition, I would like to thank Mr. Ayham Shaer who helps me to use Mathematica.

Never forget my faculty members of physics department for their help and encouragement. Finally, especial thank to my relatives and friends for their moral support and cares.

الإقرار

أنا الموقعة أدناه مقدمة الرسالة التي تحمل عنوان:

**التمغنط لزوج من النقاط الكمية (GaAs) في مجال مغناطيسي**

**The Magnetization of The (GaAs) Double  
Quantum Dots in a Magnetic Field**

أقر بأن ما اشتملت عليه هذه الرسالة، إنما هي نتاج جهدي الخاص، باستثناء ما تمت الإشارة إليه حيثما ورد، وأن هذه الرسالة ككل، أو أي جزء منها لم يقدم من قبل لنيل أي درجة علمية أو بحث علمي أو بحثي لدى أي مؤسسة تعليمية أو بحثية أخرى.

**Declaration**

The work provided in this thesis, unless otherwise referenced, is the researcher's own work, and has not been submitted elsewhere for any other degree or qualification.

Student's Name: اشتياق "محمد ياسر" حجاز اسم الطالب:

Signature: ..... اشتياق حجاز ..... التوقيع:

Date: 24/05/2016 التاريخ:

## Table of Contents

No.	Content	Page
	Dedication	III
	Acknowledgement	IV
	Declaration	V
	Table of Contents	VI
	List of Tables	VII
	List of Figures	VIII
	List of Symbols and Abbreviations	XI
	Abstract	XIII
	<b>Chapter One: Introduction</b>	1
1.1	Nanotechnology and nanoscale	1
1.2	Low Dimensional systems	2
1.3	Quantum dots	4
1.4	Literature Survey	8
1.5	Heterostructure and confinement potential	11
1.6	Research objectives	14
1.7	Thesis Layout	14
	<b>Chapter Two: Theory</b>	16
2.1	The double quantum dots Hamiltonian	16
2.2	SQD Variation of Parameter Method	18
2.3	Energy calculation spectra	19
2.4	Exact diagonalization method	24
2.5	Magnetization	25
	<b>Chapter Three: Results and Discussion</b>	26
3.1	DQD energy spectra	26
3.2	Magnetization	38
	<b>Chapter Four: Conclusion and Future Work</b>	49
	<b>References</b>	50
	<b>Appendix A<sub>1</sub></b> : Decoupling of the single quantum dot Hamiltonian	53
	<b>Appendix A<sub>2</sub></b> : The variation of parameter method of the SQD Hamiltonian	57
	<b>Appendix A<sub>3</sub></b> : Exact diagonalization technique	60
	المخلص	٦

**List of Tables**

<b>No.</b>	<b>Table Captions</b>	<b>Page</b>
Table (3.1)	The computed energy spectra of the DQD states against the magnetic field for two interacting electrons for $\omega_o = \frac{2}{3} R^*$ , $\Delta = 0.5 R^*$ , $V_o = 1R^*$ .	30

## List of Figures

No.	Figure Captions	Page
Fig. (1.1)	Schematic image and the density of state as function of energy for various confinement systems: bulk (3D), quantum well (2D), quantum wire (1D), and quantum dot (0D).	4
Fig. (1.2)	Type-I QD and type-II QD, in a Type-I QD both the holes and the electrons are confined in the dot, however, for type-II systems only the electrons (holes) are localized in the dot and the holes (electrons) remain outside the dot in the barrier material.	6
Fig. (1.3)	A double quantum dot. Each electron spin SL or SR define one quantum two-level system, or qubit. A narrow gate between the two dots can modulate the coupling, allowing swap operations.	7
Fig. (1.4)	a) Atomic force micrograph and b) schematic aerial view of two quantum dots which are defined in the two-dimensional electron system 2DES of a GaAs/AlGaAs heterostructure.	7
Fig. (1.5)	Atomic force microscope (AFM) image of a double quantum dot device, defined by metal gate electrodes on top of a GaAs/AlGaAs heterostructure.	11
Fig. (1.6)	Scanning electron microscope SEM micrograph of a sample: Surface of an AlGaAs/GaAs heterostructure (dark) with gold gates (light gray).	12
Fig. (1.7)	Schematic representation for the mechanism of confining electrons in semiconductor QD heterostructure showing a 2DEG at the interface between GaAs and AlGaAs heterostructure.	13
Fig. (3.1)	a) Our computed energy spectra of two interacting electrons in double quantum dots against the strength of the magnetic field for the range of $\omega_c = \{0, 1R^*\}$ , and angular momentum $m = 0, 1, 2$ . b) The computed energy spectra of two interacting electrons in double quantum dots in Ref [30].	28
Fig. (3.2)	The computed energy spectra of two interacting electrons in double quantum dots against the strength of the magnetic field.	29

No.	Figure Captions	Page
Fig. (3.3)	The energy of DQD for fixed values of $\omega_0 = \frac{2}{3} R^*$ , $\Delta = 0.5 R^*$ , $V_o = 1R^*$ against the number of basis and various confining cyclotron frequencies.	32
Fig. (3.4)	a) Our computed exchange energy of the two interacting electrons in DQD against the magnetic field strength. b) The computed exchange energy of the two interacting electrons in DQD against the magnetic field strength in Ref [30].	33
Fig. (3.5)	The exchange energy of the two interacting electrons in SQD against the magnetic field strength for $\omega_0 = \frac{2}{3} R^*$ results by turning off the $V_b$ - term in the DQD Hamiltonian.	34
Fig. (3.6)	Comparison between the exchange energy of the two interacting electrons in SQD results by turning off the $V_b$ - term in the DQD Hamiltonian, and the exchange energy of the two interacting electrons in DQD against the magnetic field strength.	34
Fig. (3.7)	The exchange energy of the two interacting electrons in DQD against the magnetic field strength for $\omega_0 = \frac{2}{3} R^*$ , $\Delta = 0.5 R^*$ and different values of $V_o$ .	35
Fig. (3.8)	The exchange energy of the two interacting electrons in DQD against the magnetic field strength for $V_o = 1 R^*$ , $\Delta = 0.5 R^*$ and different values of $\omega_0$ .	35
Fig. (3.9)	Phase diagrams for the exchange energy. a) The relation between $\omega_c (R^*)$ and $\omega_0 (R^*)$ at $V_o = 1 R^*$ . b) The relation between $\omega_c (R^*)$ and $V_o (R^*)$ at $\omega_0 = \frac{2}{3} R^*$ .	36
Fig. (3.10)	The statistical energy of two interacting electrons in double quantum dots against the strength of the magnetic field for $\omega_0 = \frac{2}{3} R^*$ , $\Delta = 0.5 R^*$ , $V_o = 1R^*$ .	37
Fig. (3.11)	The statistical energy of two interacting electrons in double quantum dots against the strength of the magnetic field for $\omega_0 = \frac{2}{3} R^*$ , $\Delta = 0.5 R^*$ , $V_o = 1R^*$ . The curve shows a cusp at $\omega_c = 0.5 R^*$ .	37
Fig. (3.12)	The magnetization (in unit of $\mu_B = \frac{e\hbar}{2m^*} = 0.87 \text{ meV/T}$ for GaAs) at $T = 0.01 \text{ K}$ , of the two interacting electrons in DQD against the magnetic field strength.	39

No.	Figure Captions	Page
Fig. (3.13)	The magnetization (in unit of $\mu_B = \frac{e\hbar}{2m^*} = 0.87$ meV/T for GaAs) at $T = 0.01$ K, of the two interacting electrons in SQD against the magnetic field strength results by turning off the $V_b$ - term in the DQD Hamiltonian.	40
Fig. (3.14)	Comparison between the magnetization (in unit of $\mu_B$ ) of the two interacting electrons in SQD results by turning off the $V_b$ - term in the DQD Hamiltonian, and the magnetization (in unit of $\mu_B$ ) at of the two interacting electrons in DQD against the magnetic field strength.	40
Fig. (3.15)	The magnetization (in unit of $\mu_B$ ) of the two interacting electrons in DQD against the magnetic field strength a) at $T = 0.01$ K, b) at $T = 0.1$ K, c) at $T = 1$ K and d) The three curves at the same graph.	41
Figure (3.16)	The magnetization (in unit of $\mu_B$ ) of the two interacting electrons in DQD against the magnetic field strength showing the first cusp. a) at $T = 0.01$ K , b) at $T = 0.1$ K,c) at $T = 1$ K and d) The three curves at the same graph.	43
Fig. (3.17)	The magnetization (in unit of $\mu_B$ ) of the two interacting electrons in DQD against the magnetic field strength showing the second cusp. a) at $T = 0.01$ K , b) at $T = 0.1$ K, c) at $T = 1$ K and d) The three curves at the same graph.	45
Fig. (3.18)	The magnetization (in unit of $\mu_B$ ) of the two interacting electrons in DQD against the magnetic field strength for $\omega_o = \frac{2}{3} R^*$ , $\Delta = 0.5 R^*$ . a) $V_o = 0.5 R^*$ , b) $V_o = 1 R^*$ , c) $V_o = 1.5 R^*$ and d) The three curves in one plot.	47

### List of Symbols and Abbreviations

QD	: Quantum dot
3D	: Three dimension
2D	: Two dimension
1D	: One dimension
0D	: Zero dimension (quantum dot)
SQD	: Single quantum dot
DQD	: Double quantum dots
$V_o$	: Barrier height
$V_b$	: Potential barrier
2DES	: Two-dimensional electron system
$M$	: Magnetization
$C_v$	: Heat capacity
$S$	: Spin -Singlet state
$T$	: Spin -Triplet state
$\omega_c$	: Cyclotron frequency
$\omega_o$	: Confining frequency
$B$	: Magnetic field
$\chi$	: Magnetic susceptibility
SFA	: Static fluctuation approximation
GaAs	: Gallium Arsenide
AlGaAs	: Aluminum Gallium Arsenide
DFT	: Density functional theory
AFM	: Atomic force microscope
SEM	: Scanning electron microscope
QPC	: Quantum point contacts
MBE	: Molecular beam epitaxy
n- AlGaAs	: n-type Aluminum Gallium Arsenide
$V(x,y)$	: Lateral confinement potential

$\Delta$	: Barrier width
$e$	: Charge of electron
$m^*$	: Effective mass of electron
$m_e$	: mass of electron
$\mathbf{r}_j$	: Position of the electron inside the QD
$\mathbf{p}(\mathbf{r}_j)$	: Momentum of the electron inside the QD
$p(r)$	: The linear momentum
R	: Center of mass position
r	: Relative motion position
A(r)	: Vector potential
c	: Speed of light
$\epsilon$	: The dielectric constant of material
$\mu$	: Reduced mass
$R^*$	: Effective Rydberg unit
$\hbar$	: Reduced Planck's constant
$\alpha$	: Effective frequency
$i$	: Imaginary number
$\Psi$	: Wave function
K	: Kelvin Degree
T	: Temperature
n	: Principle quantum number
m	: Angular quantum number
$V_{eff}$	: Effective potential

**The Magnetization of The (GaAs) Double  
Quantum Dots in a Magnetic Field**

**By**

**Eshtiaq "Mohammed Yasir" Hijaz**

**Supervisor**

**Prof.Dr. Mohammad Elsaid**

**Co-supervisor**

**Dr. Musa Elhasan**

**Abstract**

The magnetization of two interacting electrons confined in double quantum dots under the effect of an applied uniform magnetic field along z-direction, in addition to a Gaussian barrier had been calculated. The variational and exact diagonalization methods had been used to solve the Hamiltonian and compute the magnetization of the double quantum dots. In addition, we had investigated the dependence of the magnetization on temperature, magnetic field, confining frequency, barrier height and barrier width. The singlet-triplet transitions in the ground state of the double quantum dots spectra and the corresponding jumps in the magnetization curves had also been shown. The comparisons show that our results are in very good agreement with reported works.

## **Chapter One**

### **Introduction**

#### **1.1 Nanotechnology and nanoscale:**

A generalized description of nanotechnology was subsequently established by the National Nanotechnology Initiative, which defines nanotechnology as the manipulation of matter with at least one dimension sized from 1 to 100 nanometers. This definition reflects the fact that quantum mechanical effects are important at this quantum-realm scale [1].

Nanotechnology as defined by size is naturally very broad, including fields of science such as surface science, organic chemistry, molecular biology, semiconductor physics, microfabrication, etc.

Scientists currently debate the future implications of nanotechnology. Nanotechnology may be able to create many new materials and devices with a vast range of applications, such as in medicine, electronics and biomaterials energy production.

The nanoscopic scale (or nanoscale) usually refers to structures with a length scale applicable to nanotechnology, usually cited as 1–100 nanometers.

For technical purposes, the nanoscopic scale is the size at which fluctuations in the averaged properties (due to the motion and behavior of

individual particles) begin to have a significant effect on the behavior of a system, and must be taken into account in its analysis.

The nanoscopic scale is sometimes marked as the point where the properties of a material change, above this point, the properties of a material are caused by bulk or volume effects. Below this point the surface area effects (also referred to as quantum effects) become more apparent, these effects are due to the geometry of the material, which can have a drastic effect on quantized states, and thus the properties of a material.

### **1.2 Low dimensional system:**

Low dimensional systems refer to those systems in which at least one of the three dimensions is intermediate between those characteristic of atoms/molecules and those of the bulk material, generally in the range from 1 nm to 100 nm, so the motion of charge carriers such as electrons is restricted from exploring the full three dimensions. Those systems can have very high surface area to volume ratio. Consequently, the surface states become important and even dominant. In addition, the dimensional constraint on the system gives rise to quantum size effects, which can significantly change the energy spectrum of electrons and their behavior. As a result, some properties of such systems are very different from those of their bulk counterparts. Those systems have shown extraordinary electronic, optical, thermal, mechanical and chemical properties, which may result in their use in wide range of nanotechnology.

Low dimensional systems such as quantum dots, quantum wires and quantum wells are semiconductors whose size confine the charge carriers in a limited size (few nanometers) in three, two and one dimension respectively. The confinement phenomena change significantly the density of state of the system and the energy spectra. For quantum dot (zero dimensional system) the density of state shows a discrete behavior unlike to the other confinements which have a continuous density of state, so QDs have fully quantized energy levels due to its three dimensional confinement. The density of state for these confinements are shown in Figure (1.1).

The nanofabrication techniques allow us to control precisely both the size and the shape of the low dimensional system.

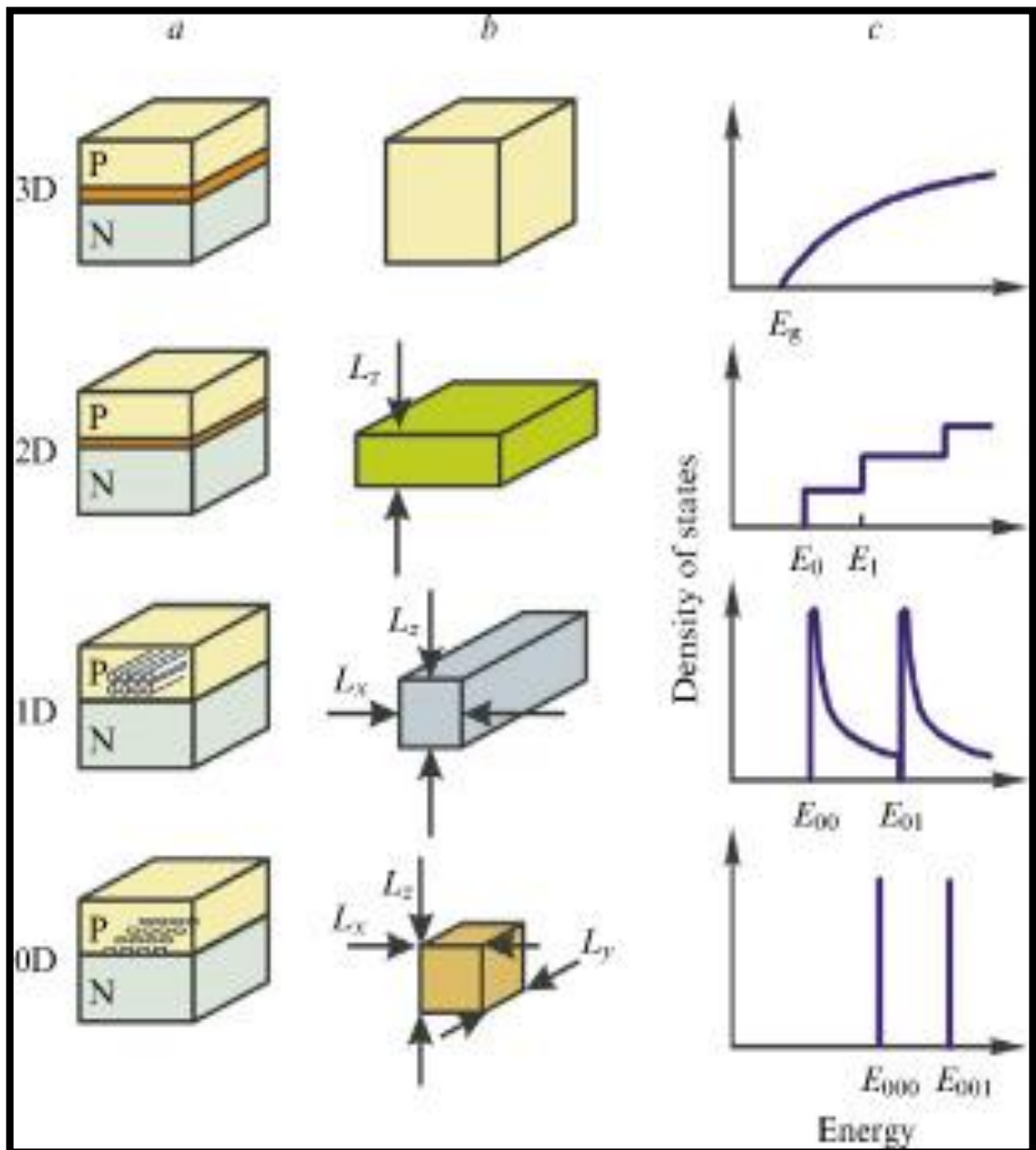


Figure (1.1): Schematic image and the density of state as function of energy for various confinement systems: bulk (3D), quantum well (2D), quantum wire (1D), and quantum dot (0D).

### 1.3 Quantum dots:

Quantum dots (QDs) are nanostructures that confine the carriers (electrons and holes) in three spatial dimensions, thus QD has zero degree of freedom. Due to this confinement of the electrons the energy spectra are fully quantized. There are two types of QDs as explained in figure (1.2).

In early 1980s, the first QD were successfully made in laboratory, this forced to investigate the properties of the quantum dot system and to study the effect of the size, material, and shape.

Quantum dot is often called the artificial atoms due to its similarity with real atom. Electrons in both real and artificial atoms are attracted to a central potential, in natural atom this is a positively charged nucleus, while in artificial atom these electrons are trapped in a bowl-like parabolic potential. Moreover, the number of electrons in atoms can be tuned by ionization, while in QDs the number of electrons is tuned by changing the confinement potential.

Current nanofabrication methods allow us to control precisely both the size and the shape of the QD. The electronic characteristics of a quantum dot are closely related to its size and shape. The size of the QDs is about 100 nm in diameter.

The QDs can be fabricated by two different ways, the first one is made by using lithography techniques of microchip manufacturing; and the second approach can be done by applying chemical processes to get a QD from bulk material [1,2].

Due to the structural, optical and transport properties of the QD it has a wide range of application in different aspects such as: laser devices, memories, single electron transistor (SET) [3], solar cell with high

efficiency, spin-based quantum computer shown in figure (1.4) [4, 5] , amplifiers and sensors.

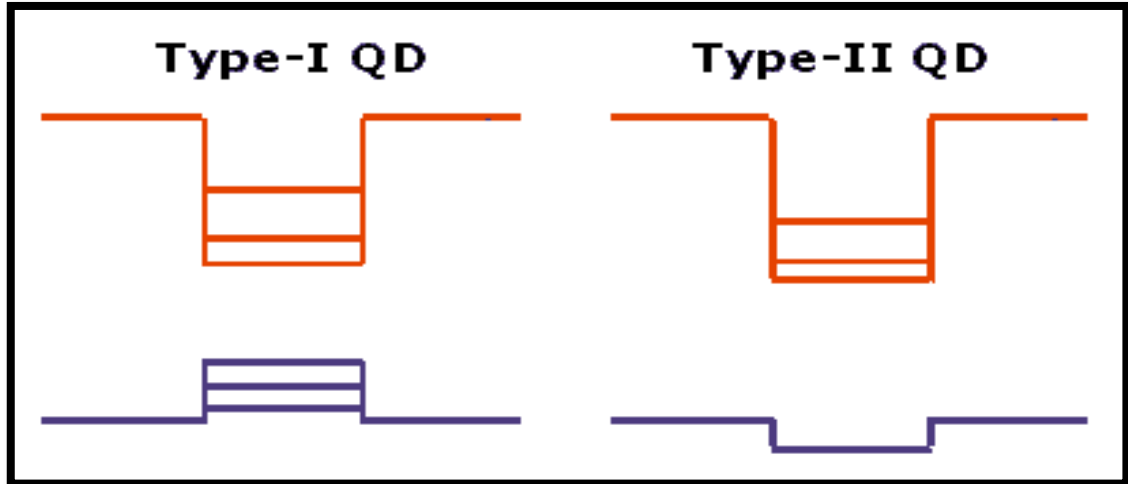


**Figure (1.2): Type-I QD and type-II QD, in a Type-I QD both the holes and the electrons are confined in the dot, however, for type-II systems only the electrons (holes) are localized in the dot and the holes (electrons) remain outside the dot in the barrier material.**

In recent years, there has been great interest in the double quantum dots (DQD) system. The double quantum dots system consists of two single quantum dots separated by a potential barrier of height  $V_o$  which can be tuned so the nature of the interaction between the two electrons which are confined in each single quantum dot (SQD) can be changed by this tuning potential. Turning off the potential barrier ( $V_b = 0$ ), in this case the DQD will be reduced to the SQD. The DQD system is shown in figure (1.4).

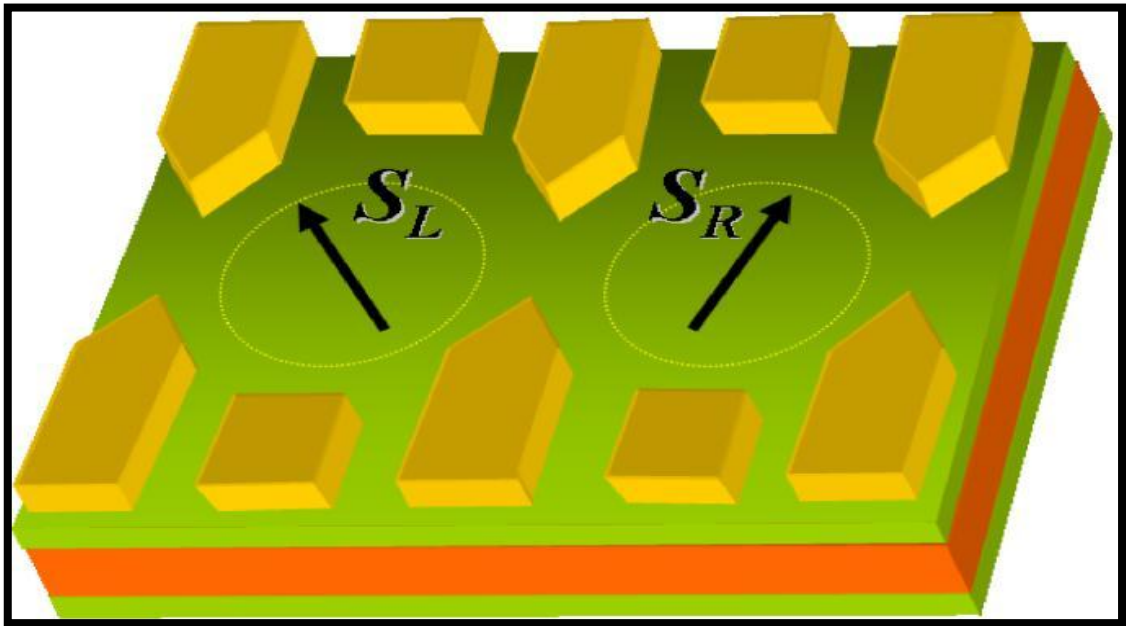


Figure (1.3): A double quantum dot. Each electron spin  $S_L$  or  $S_R$  define one quantum two-level system, or qubit. A narrow gate between the two dots can modulate the coupling, allowing swap operations.

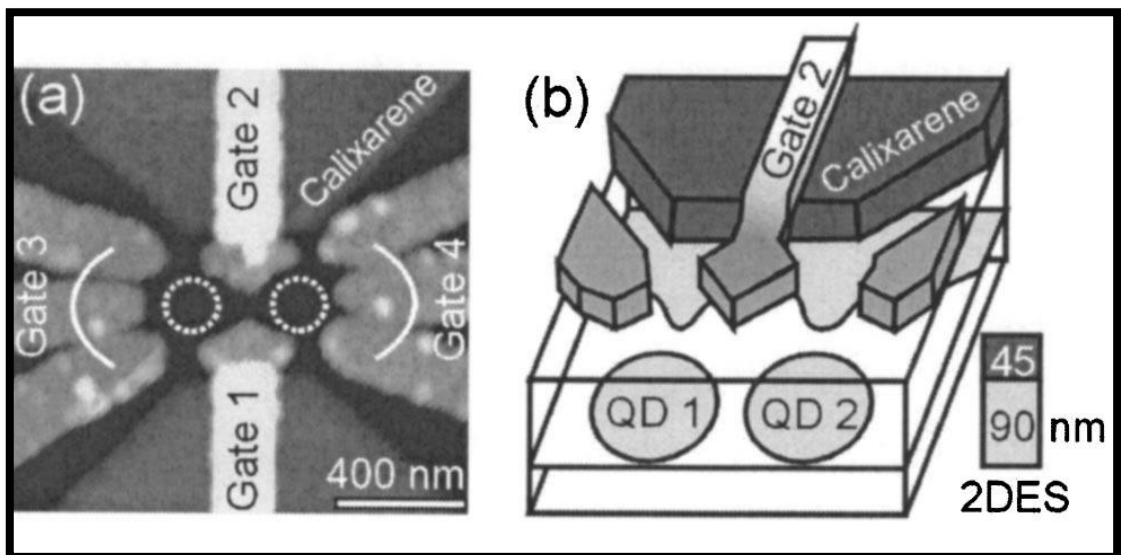


Figure (1.4): a) Atomic force micrograph and b) schematic aerial view of two quantum dots which are defined in the two-dimensional electron system 2DES of a GaAs/AlGaAs heterostructure.

#### 1.4 Literature survey:

The electronic structure of the quantum dots depend strongly on the interplay between electron-electron interaction (coulomb energy), confining potential, and the applied magnetic field. The existence of both coulomb and parabolic potentials make the analytical solution of the quantum dot's Hamiltonian is not attainable. Different theoretical techniques had been used to solve the two electrons' quantum dot Hamiltonian, to obtain the eigenenergies and eigenstates of the system [6-18].

Wagner, Merkt and Chaplik [6] had studied this interesting QD system and predicted the oscillations between spin-singlet (S) and spin-triplet (T) ground states.

Taut [7] had managed to obtain the exact analytical results for the energy spectrum of two interacting electrons through a coulomb potential, confined in a QD, just for particular values of the magnetic field strength. In references [8, 9] the authors had solved the QD-Hamiltonian by variational method and obtained the ground state energies for various values of magnetic field ( $\omega_c$ ), and confined frequency ( $\omega_0$ ). In addition, they had performed exact numerical diagonalization for the Helium QD-Hamiltonian and obtained the energy spectra for zero and finite values of magnetic field strength. Kandemir [10, 11] had found the closed form solution for this QD Hamiltonian and the corresponding eigenstates for particular values of the magnetic field strength and confinement

frequencies. Elsaid [12, 13, 14, 15, and 16] had used the dimensional expansion technique, in different works, to study and solve the QD-Hamiltonian and obtain the energies of the two interacting electrons for any arbitrary ratio of coulomb to confinement energies and gave an explanation to the level crossings.

Maksym and Chakraborty [17] had used the diagonalization method to obtain the eigenenergies of interacting electrons in a magnetic field and show the transitions in the angular momentum of the ground states. They had also calculated the heat capacity curve for both interacting and non-interacting confined electrons in the QD presented in a magnetic field. The interacting model shows very different behavior from non-interacting electrons, and the oscillations in these magnetic and thermodynamic quantities like magnetization ( $M$ ) and heat capacity ( $C_v$ ) are attributed to the spin singlet-triplet transitions in the ground state spectra of the quantum dot. De Groote, Hornos and Chaplik [18] had also calculated the magnetization( $M$ ), susceptibility( $\chi$ ) and heat capacity( $C_v$ ) of helium like confined QDs and obtained the additional structure in magnetization. In a detailed study, Nguyen and Peeters [19] had considered the QD helium in the presence of a single magnetic ion and applied magnetic field taking into account the electron-electron correlation in many quantum dots. They had shown the dependence of these thermal and magnetic quantities:  $C_v$ ,  $M$  and  $\chi$  on the strength of the magnetic field, confinement frequency, magnetic ion position and temperature. They had observed that the cusps in the energy levels show up as peaks in the heat capacity and magnetization.

In reference [20], the authors had used the static fluctuation approximation (SFA) to study the thermodynamic properties of two dimensional GaAs/AlGaAs parabolic QD in a magnetic field.

Boyacioglu and Chatterjee [21] had studied the magnetic properties of a single quantum dot confined with a Gaussian potential model. They observed that the magnetization curve shows peaks structure at low temperature. Helle, Harju and Nieminen [22] had computed the magnetization of a rectangular QD in a high magnetic field and the results show the oscillation and smooth behavior in the magnetization curve for both, interacting and non-interacting confined electrons, respectively.

In an experimental work [23], the magnetization of electrons in GaAs/AlGaAs semiconductor QD as function of applied magnetic field at low temperature 0.3 K had been measured. They had observed oscillations in the magnetization. To reproduce the experimental results of the magnetization, they found that the electron-electron interaction should be taken into account in the theoretical model of the QD magnetization.

Furthermore, the density functional theory (DFT) had been used to investigate the magnetization of a rectangular QD in the applied external magnetic field [24].

Climente, *Planelles and Movilla* had studied the effect of coulomb interaction on the magnetization of quantum dot with one and two interacting electrons [25].

Very recently, Avetisyan, Chakraborty and Pietilainen [26] had studied the magnetization of anisotropic QD in the presence of the Rashba spin-orbit interaction for three interacting electrons in the dot.

### **1.5 Heterostructure and confinement potential:**

As we mentioned, the nanofabrication methods enable us to fabricate electronic structures where the electrons are confined in a small regions of the order of nanometers QDs. The QD is a small island on a semiconductor heterostructure, where the shape QD and the number of the electrons can be controlled by an external voltage. An atomic force microscope image of a double quantum dot device is shown in figure (1.5).

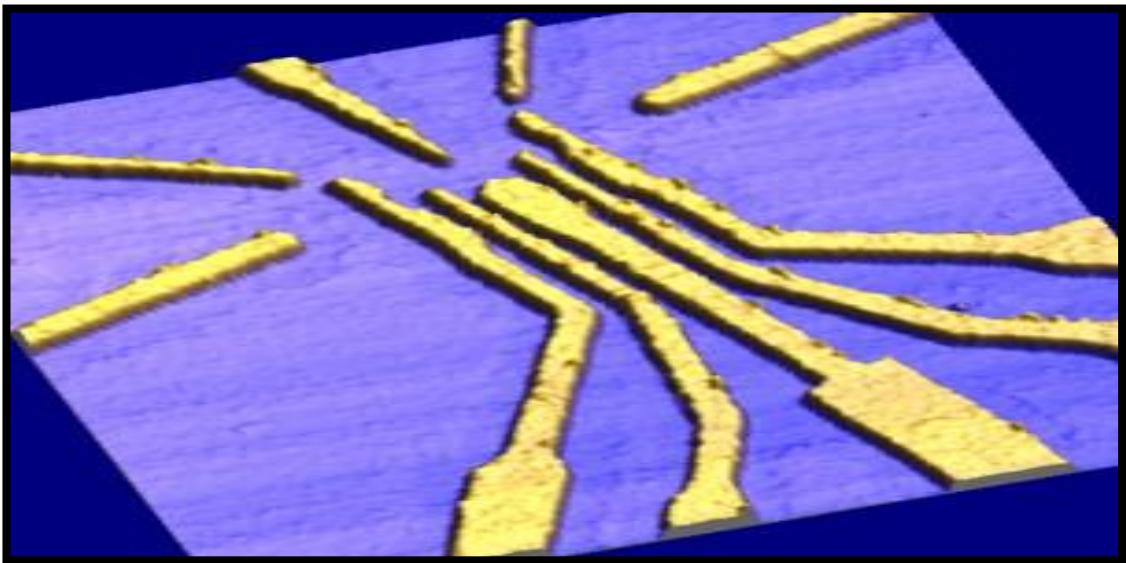


**Figure (1.5): AFM(atomic force microscope) image of a double quantum dot device, defined by metal gate electrodes on top of a GaAs/AlGaAs heterostructure. Constrictions on both sides of the quantum dots form quantum point contacts, which can be operated as charge detectors.**

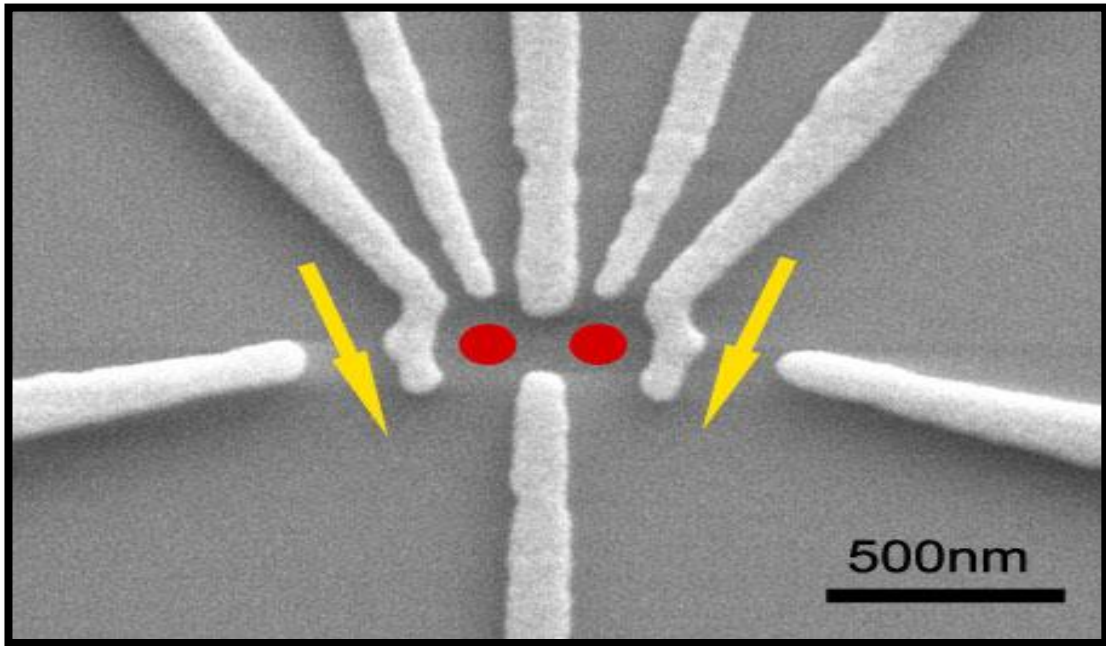


**Figure (1.6):** Scanning electron microscope SEM micrograph of a sample: Surface of an AlGaAs/GaAs heterostructure (dark) with gold gates (light gray), that allow to locally deplete the 2DES and thus define two tunnel double quantum dots (red) and two quantum point contacts (QPC) on the sides.

The DQD are fabricated from GaAs/AlGaAs semiconductor heterostructure. The heterostructure is growing by the molecular beam epitaxy (MBE) method.

The AlGaAs layer is doped with Si donors to have free electrons in the heterostructure (n type AlGaAs). The free electrons translate from AlGaAs layer which has high band gap to GaAs layer with lower band gap. After that the free electrons are trapped in the quantum well of GaAs layer. By this a 2D structure is created, in this structure the motion of the electrons is quantized along growth axis (z direction) while the motion of the electron in xy plane (n substrate) is free as shown in figure (1.7).

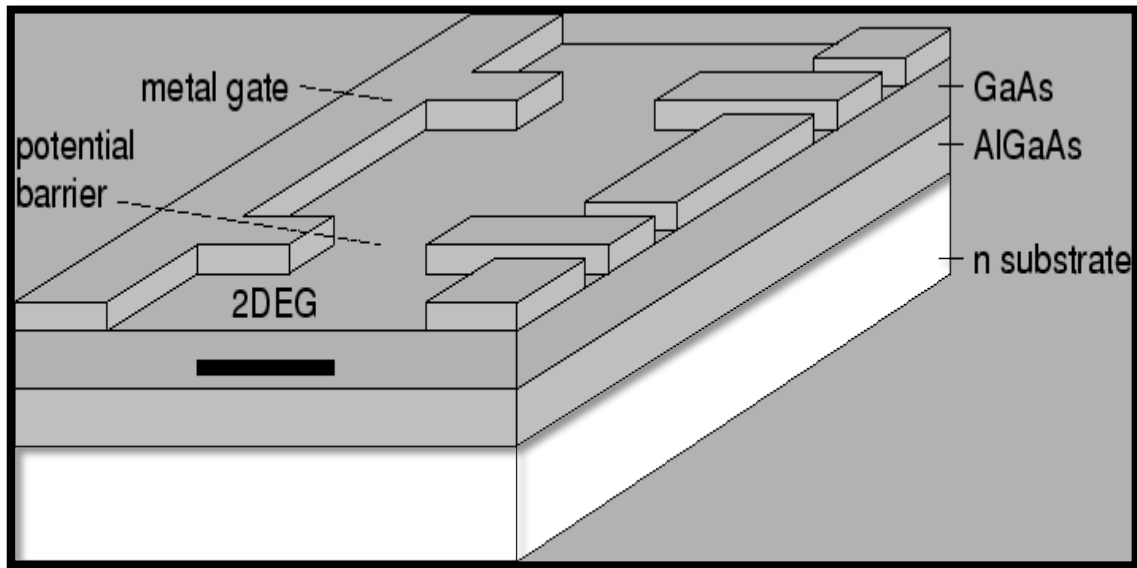


**Figure (1.7): Schematic representation for the mechanism of confining electrons in semiconductor QD heterostructure showing a 2DEG at the interface between GaAs and AlGaAs heterostructure. The electrons in the 2DEG is due to the ionization of silicon donors located in the n-AlGaAs layer.**

Finally a negative voltage is applied on the surface of the heterostructure to reduce further the confinement region and create one or more small islands from large two dimensional electron gas (2DEG).

The lateral confinement potential  $V(x,y)$  is quite similar to the coulomb potential which confines the electrons in the real atoms, therefore the QD is called an artificial atom. The confinement potential is usually taken to be a simple parabolic model, the theoretical-experimental comparisons show that the harmonic oscillator model is the best model to describe this confinement.

## 1.6 Objectives:

This thesis has two objectives which can be summarized as follows:

- 1) Variational and exact diagonalization methods will be used to solve the DQD Hamiltonian and obtain the desired energy spectra of the system. The complete energy spectra of DQD will be calculated as function of confinement frequency ( $\omega_o$ ), strength of magnetic field ( $\omega_c$ ), barrier height ( $V_o$ ) and barrier width ( $\Delta$ ).
- 2) The computed energy spectra of the double quantum dots system will be used to calculate the magnetization (M). The behavior of the magnetization will be displayed as a function of the temperature (T), magnetic strength ( $\omega_c$ ), confining potential ( $\omega_o$ ), the width of the barrier ( $\Delta$ ) and the height of the barrier ( $V_o$ ).

## 1.7 Outlines of thesis:

In this work, the magnetization of DQD system has been calculated as a thermodynamic quantity of the system in which both the magnetic field and the electron-electron interaction are fully taken into account. Since, the eigenvalues of the electrons in the DQD are the starting point to calculate the physical properties of the DQD system, the variational and the exact diagonalization methods have been used to solve the DQD Hamiltonian and obtain the eigenenergies. Second, the eigenenergies spectra had been calculated to display theoretically the behavior of the magnetization of the DQD as a function of magnetic field strength,

confining frequency, the width of the barrier, the height of the barrier and temperature.

The rest of this thesis is organized as follows: the Hamiltonian theory, the principle of the variation of parameter technique and how to calculate the magnetization of the DQD system from the mean energy expression are presented in chapter II. In chapter III, the results of energy and magnetization of our work had been displayed and discussed, while the final chapter devoted for conclusions and future work.

## Chapter Two

### Theory

This chapter consists of four main parts : The DQD Hamiltonian, the variation theory, the exact diagonalization technique and the magnetization.

#### 2.1 The double quantum dots Hamiltonian:

Consider two interacting electrons inside double quantum dots confined by a parabolic potential of strength  $\omega_o$  under the effect of an applied uniform magnetic field of strength  $\omega_c$ , taken to be along z-direction, in addition to a Gaussian barrier of width  $\Delta$  and height  $V_o$ . This model can be characterized by the Hamiltonian ( $H_{DQD}$ ),

$$H_{DQD} = \sum_{j=1}^2 \left\{ \frac{1}{2m^*} \left[ \mathbf{p}(\mathbf{r}_j) + \frac{e}{c} \mathbf{A}(\mathbf{r}_j) \right]^2 \right\} + \frac{1}{2} m^* \omega_o^2 r_j^2 + \frac{e^2}{\epsilon |r_1 - r_2|} + V_o (e^{-x_1^2/\Delta^2} + e^{-x_2^2/\Delta^2}). \quad (2.1)$$

Where  $\mathbf{r}_j$  and  $\mathbf{p}(\mathbf{r}_j)$  are the position and momentum of the electron inside the QD. In addition,  $x_1$  and  $x_2$  represent the position of each quantum dot along the  $x$  –direction.

$H_{DQD}$  can be considered as the sum of the single quantum dot Hamiltonian ( $H_{SQD}$ ) and the potential barrier term  $V_b = V_o (e^{-x_1^2/\Delta^2} + e^{-x_2^2/\Delta^2})$  as follows,

$$H_{DQD} = H_{SQD} + V_b. \quad (2.2)$$

Initially, we have emphasized that the SQD-Hamiltonian had been solved variationally in a previous study. The  $V_b$ -term will be turned off to compute the eigenenergies of the single quantum dot case. The Hamiltonian ( $H_{SQD}$ ) can be separated to a Center of mass and relative motion Hamiltonians.

The Hamiltonian for two interacting electrons confined in a single quantum dot by a parabolic potential in a uniform magnetic field of strength  $\omega_c$ , applied along z direction is given in appendix  $A_1$ .

The single quantum dot Hamiltonian ( $H_{SQD}$ ) can be decoupled into center of mass ( $H_{CM}$ ) and relative ( $H_r$ ) parts as shown in the appendix  $A_1$ .

$$H_{SQD} = H_{CM} + H_r. \quad (2.3)$$

The energy of the  $H_{SQD}$  can be written as:

$$E_{SQD} = E_{CM} + E_r. \quad (2.4)$$

The center of mass part of the SQD Hamiltonian has the well known harmonic oscillator form for the wave function and energy, this form was found Independently by Fock [27] and Darwin [28] as presented in appendix  $A_1$

The relative part of the SQD Hamiltonian does not have an analytical solution for all ranges of  $\omega_0$  and  $\omega_c$  because of both coulomb and parabolic terms in the  $H_{SQD}$ , so the relative Hamiltonian part had been solved

variationally in terms of a variational parameter to obtain the energy spectra.

The effective frequency is the sum of a nanostructure confining frequency and the magnetic field confining frequency, using a new parameter ( $\alpha$ ) defined as follow

$$\alpha = \frac{1}{4} \sqrt{\frac{\omega_c^2}{4} + \omega_0^2} \quad (2.5)$$

Finally, To find the full energy spectra of the DQD system the energy matrix elements of the barrier term will be computed using the variational method. The combined terms of the single quantum dot Hamiltonian energy and barrier energy matrix elements will be diagonalized to give the full matrix elements of the DQD Hamiltonian.

## 2.2 SQD variation of parameter method:

The variational method will be used as an approximation method to calculate the desired energy eigenvalues of the relative part Hamiltonian of the single quantum dot Hamiltonian.

The adopted one parameter variational wave function is :

$$\psi(r) = \sqrt[4]{\alpha} \frac{u_m(\rho) e^{im\phi}}{\sqrt{2\pi} \sqrt{\rho}} \quad (2.6)$$

Where,  $\rho = \sqrt{\alpha} r$  (2.7)

We have normalized our wave function

$$u_m(\rho) = C_m \rho^{1/2+|m|} (1 + \beta\rho) e^{-\left(\frac{\rho^2}{2}\right)} \quad (2.8)$$

The above normalization constant can be expressed in terms of new constants as given in the appendix  $A_2$

The energies of the relative part of the single quantum dot Hamiltonian can be obtained by calculating the energy matrix elements  $E_r = \langle \psi | H_r | \psi \rangle$  as expressed in appendix  $A_2$ .

The energy eigenvalues of  $H_r$  can be computed by minimizing the energy formula with respect to the variational parameter  $\beta$ , which is given in appendix  $A_2$ .

### 2.3 energy calculations spectra:

Now, to compute the full energy spectra of the DQD system we have set  $V_o > 0$  in the Hamiltonian model equation (2.1), so the potential of the barrier is

$$V_b = V_o \left( e^{-x_1^2/\Delta^2} + e^{-x_2^2/\Delta^2} \right) \quad (2.9)$$

Coupling the center of mass and the relative motion, so the variational wave function has been chosen as products

$$U_m = u_m(\rho, \varphi) \Psi_o(\vec{R}) \quad (2.10)$$

$$u_m(\rho, \varphi) = u_{m,\beta_m}(\rho) \frac{e^{im\varphi}}{\sqrt{2\pi}} \quad (2.11)$$

The center of mass wave function is the Fock Darwin ground state

$$\Psi_o(\vec{R}) = 2 \sqrt{\frac{\alpha}{\pi}} e^{-2\alpha R^2} \quad (2.12)$$

The matrix elements  $H_{m,n} = \langle U_m | H | U_n \rangle$  have been found, and to this goal the effective potential is  $V_{eff}(\rho, \varphi) = \langle \Psi_o | V_b | \Psi_o \rangle$ .

$$V_{eff}(\rho, \varphi) = \frac{2V_o\gamma}{\sqrt{\gamma^2+1}} e^{-(\rho^2 \cos^2 \varphi)/(\gamma^2+1)} \quad (2.13)$$

Where  $= 2 \Delta \sqrt{\alpha}$ .

Evaluating the matrix elements of the effective potential  $\langle u_m | V_{eff} | u_n \rangle$  where,

$$u_m(\rho, \varphi) = u_{m,\beta_m}(\rho) \frac{e^{im\varphi}}{\sqrt{2\pi}}. \quad (2.14)$$

$$u_m(\rho, \varphi) = C_{m,\beta_m} \rho^{1/2+|m|} (1 + \beta_m \rho) e^{-\left(\frac{\rho^2}{2}\right)} \frac{e^{im\varphi}}{\sqrt{2\pi}}. \quad (2.15)$$

Then,

$$\langle u_m | V_{eff} | u_n \rangle = \int_0^{2\pi} \int_0^\infty u_m(\rho, \varphi)^* V_{eff} u_n(\rho, \varphi) d\rho d\varphi. \quad (2.16)$$

$$\langle u_m | V_{eff} | u_n \rangle =$$

$$\int_0^{2\pi} \int_0^\infty C_{m,\beta_m} \rho^{1/2+|m|} (1 + \beta_m \rho) e^{-\left(\frac{\rho^2}{2}\right)} \frac{e^{-im\varphi}}{\sqrt{2\pi}} \times$$

$$\frac{2V_o\gamma}{\sqrt{\gamma^2+1}} e^{-(\rho^2 \cos^2 \varphi)/(\gamma^2+1)} C_{n,\beta_n} \rho^{1/2+|n|} (1$$

$$+ \beta_n \rho) e^{-\left(\frac{\rho^2}{2}\right)} \frac{e^{in\varphi}}{\sqrt{2\pi}} d\rho d\varphi. \quad (2.17)$$

$$= C_{m,\beta_m} C_{n,\beta_n} \frac{2V_0\gamma}{\sqrt{\gamma^2+1}} \frac{1}{2\pi} \int_0^{2\pi} \int_0^\infty \rho^{1/2+|m|} \rho^{1/2+|n|} (1 + \beta_m \rho) (1 + \beta_n \rho) \times \\ e^{-\left(\frac{\rho^2}{2}\right)} e^{-\left(\frac{\rho^2}{2}\right)} e^{-(\rho^2 \cos^2 \varphi)/(\gamma^2+1)} e^{i(n-m)\varphi} d\rho d\varphi. \quad (2.18)$$

$$= C_{m,\beta_m} C_{n,\beta_n} \frac{2V_0\gamma}{\sqrt{\gamma^2+1}} \frac{1}{2\pi} \int_0^{2\pi} \int_0^\infty [\rho^{1+|m|+|n|} e^{-\rho^2\left(1+\frac{\cos^2\varphi}{\gamma^2+1}\right)} \times \\ (1 + (\beta_m + \beta_n)\rho + \beta_m\beta_n\rho^2) d\rho] e^{i(n-m)\varphi} d\varphi. \quad (2.19)$$

$$= V_0 C_{m,\beta_m} C_{n,\beta_n} \frac{2\gamma}{\sqrt{\gamma^2+1}} \frac{1}{2\pi} \int_0^{2\pi} \left[ \int_0^\infty \rho^{1+|m|+|n|} e^{-\rho^2\left(1+\frac{\cos^2\varphi}{\gamma^2+1}\right)} d\rho + \right. \\ \left. (\beta_m + \beta_n) \int_0^\infty \rho^{2+|m|+|n|} e^{-\rho^2\left(1+\frac{\cos^2\varphi}{\gamma^2+1}\right)} d\rho + \right. \\ \left. \beta_m\beta_n \int_0^\infty \rho^{3+|m|+|n|} e^{-\rho^2\left(1+\frac{\cos^2\varphi}{\gamma^2+1}\right)} d\rho \right] e^{i(n-m)\varphi} d\varphi. \quad (2.20)$$

Let  $\rho^2 = u$  ,  $\rho = \sqrt{u}$

$$2 \rho d\rho = du.$$

$$\text{Then, } \rho^{|m|+|n|} = (u^{1/2})^{|m|+|n|} = u^{(|m|/2+|n|/2)}.$$

So,

$$\langle u_m | V_{eff} | u_n \rangle =$$

$$V_0 C_{m,\beta_m} C_{n,\beta_n} \frac{\gamma}{\sqrt{\gamma^2+1}} \frac{1}{2\pi} \int_0^{2\pi} \left[ \int_0^\infty u^{(|m|/2+|n|/2)} e^{-u\left(1+\frac{\cos^2\varphi}{\gamma^2+1}\right)} du \right. \\ \left. + (\beta_m + \beta_n) \int_0^\infty u^{(1/2+|m|/2+|n|/2)} e^{-u\left(1+\frac{\cos^2\varphi}{\gamma^2+1}\right)} du \right]$$

$$+\beta_m\beta_n \int_0^\infty u^{(1+|m|/2+|n|/2)} e^{-u\left(1+\frac{\cos^2\varphi}{\gamma^2+1}\right)} du ] e^{i(n-m)\varphi} d\varphi. \quad (2.21)$$

Let  $y = \left(1 + \frac{\cos^2\varphi}{\gamma^2+1}\right)u$ ,  $u = \frac{y}{\left(1+\frac{\cos^2\varphi}{\gamma^2+1}\right)}$  then  $dy = \left(1 + \frac{\cos^2\varphi}{\gamma^2+1}\right) du$ .

So,

$$\begin{aligned} \langle u_m | V_{eff} | u_n \rangle = \\ V_0 C_{m,\beta_m} C_{n,\beta_n} \frac{\gamma}{\sqrt{\gamma^2+1}} \frac{1}{2\pi} \int_0^{2\pi} [ \left(1 + \frac{\cos^2\varphi}{\gamma^2+1}\right)^{-(1+|m|/2+|n|/2)} \times \\ \int_0^\infty y^{(|m|/2+|n|/2)} e^{-y} dy ) + \left(1 + \frac{\cos^2\varphi}{\gamma^2+1}\right)^{-(3/2+|m|/2+|n|/2)} \times \\ (\beta_m + \beta_n) \int_0^\infty y^{(1/2+|m|/2+|n|/2)} e^{-y} dy ) + \\ \left(1 + \frac{\cos^2\varphi}{\gamma^2+1}\right)^{-(2+|m|/2+|n|/2)} \beta_m\beta_n \int_0^\infty y^{(1+|m|/2+|n|/2)} \times \\ e^{-y} dy ) ] e^{i(n-m)\varphi} d\varphi. \end{aligned} \quad (2.22)$$

Using the definition of Gamma function

$$\Gamma(t) = \int_0^\infty x^{t-1} e^{-x} dx. \quad (2.23)$$

$\langle u_m | V_{eff} | u_n \rangle =$

$$\begin{aligned} V_0 C_{m,\beta_m} C_{n,\beta_n} \frac{\gamma}{\sqrt{\gamma^2+1}} \frac{1}{2\pi} \left( \Gamma \left[ \frac{2+|m|+|n|}{2} \right] \int_0^{2\pi} \left(1 + \frac{\cos^2\varphi}{\gamma^2+1}\right)^{-(1+|m|/2+|n|/2)} e^{i(n-m)\varphi} d\varphi \right. \\ \left. + \frac{\cos^2\varphi}{\gamma^2+1} \right)^{-(1+|m|/2+|n|/2)} e^{i(n-m)\varphi} d\varphi \end{aligned}$$

$$\begin{aligned}
& +(\beta_m + \beta_n) \Gamma \left[ \frac{3 + |m| + |n|}{2} \right] \int_0^{2\pi} \left( 1 + \frac{\cos^2 \varphi}{\gamma^2 + 1} \right)^{-(3/2 + |m|/2 + |n|/2)} e^{i(n-m)\varphi} d\varphi \\
& + \beta_m \beta_n \Gamma \left[ \frac{4 + |m| + |n|}{2} \right] \times \\
& \int_0^{2\pi} \left( 1 + \frac{\cos^2 \varphi}{\gamma^2 + 1} \right)^{-(2 + |m|/2 + |n|/2)} e^{i(n-m)\varphi} d\varphi. \tag{2.24}
\end{aligned}$$

$$\begin{aligned}
& = V_0 C_{m,\beta_m} C_{n,\beta_n} \frac{\gamma}{\sqrt{\gamma^2 + 1}} \left( \Gamma \left[ \frac{2 + |m| + |n|}{2} \right] \frac{1}{2\pi} \times \right. \\
& \int_0^{2\pi} \frac{e^{i(n-m)\varphi}}{\left( 1 + \frac{\cos^2 \varphi}{\gamma^2 + 1} \right)^{-\left( \frac{2 + |m| + |n|}{2} \right)}} d\varphi + (\beta_m + \beta_n) \Gamma \left[ \frac{3 + |m| + |n|}{2} \right] \frac{1}{2\pi} \times \\
& \int_0^{2\pi} \frac{e^{i(n-m)\varphi}}{\left( 1 + \frac{\cos^2 \varphi}{\gamma^2 + 1} \right)^{-\left( \frac{3 + |m| + |n|}{2} \right)}} d\varphi + \beta_m \beta_n \Gamma \left[ \frac{4 + |m| + |n|}{2} \right] \frac{1}{2\pi} \times \\
& \left. \int_0^{2\pi} \frac{e^{i(n-m)\varphi}}{\left( 1 + \frac{\cos^2 \varphi}{\gamma^2 + 1} \right)^{-\left( \frac{4 + |m| + |n|}{2} \right)}} d\varphi. \right. \tag{2.25}
\end{aligned}$$

$$\langle u_m | V_{eff} | u_n \rangle =$$

$$\begin{aligned}
& V_0 C_{m,\beta_m} C_{n,\beta_n} \frac{\gamma}{\sqrt{\gamma^2 + 1}} \left[ K \left( (\gamma^2 + 1), \left( \frac{2 + |m| + |n|}{2} \right), n - m \right) \right. \\
& + (\beta_m + \beta_n) K \left( (\gamma^2 + 1), \left( \frac{3 + |m| + |n|}{2} \right), n - m \right) \\
& \left. + \beta_m \beta_n K \left( (\gamma^2 + 1), \left( \frac{4 + |m| + |n|}{2} \right), -m \right) \right] \tag{2.26}
\end{aligned}$$

Where

$$K(x, k, l) = \Gamma[k] (1/2\pi) \int_0^{2\pi} \left\{ [e^{il\varphi} / [1 + (1/x)\cos^2\varphi]]^k \right\} d\varphi, \quad (2.27)$$

$$x = \gamma^2 + 1,$$

$$l = n - m,$$

$$k \text{ is the power of } \left( 1 + \frac{s^2\varphi}{\gamma^2 + 1} \right).$$

The integral  $K(x, k, l)$  has been evaluated numerically.

#### 2.4 Exact diagonalization technique:

The combined terms of the single quantum dot Hamiltonian energy  $E_{SQD} = [(E_m(\beta_m)) + E_{CM}]$  and barrier energy matrix elements  $\langle u_m | V_b | u_n \rangle$  will be diagonalized to give the full matrix elements of the DQD Hamiltonian as follows :

$$H_{m,n} = [E_m(\beta_m) + E_{CM}]\delta_{m,n} + \langle u_m | V_b | u_n \rangle. \quad (2.28)$$

Where,

$$E_{CM} = (2n_{cm} + |m_{cm}| + 1)\hbar\omega_{eff} + m_{cm} \frac{\hbar\omega_c}{2}, \quad (2.29)$$

$n_{cm}$  is the radial quantum number,

$m_{cm}$  is the angular quantum number,

$$\omega_{eff} = \sqrt{\omega_o^2 + \left(\frac{\omega_c}{2}\right)^2}, \quad \omega_c = \frac{eB}{m^*}.$$

Having obtained the eigenenergies for the DQD system, now we are able to calculate the exchange energy ( $J$ ) define as:

$$J = E_{triplet} - E_{singlet} \quad (2.30)$$

For any range magnetic field, confining potential and barrier potential.

### 2.5 Magnetization:

The Magnetization is a description of how magnetic materials react to a magnetic field.

We have computed energies of the DQD system as essential data to calculate the magnetization ( $M$ ) of the DQD.

The magnetization of the DQD system is evaluated as the magnetic field derivative of the mean energy of the DQD.

$$M(T, B, \omega_o, V_o, \Delta) = \frac{-\partial \langle E(T, B, \omega_o, V_o, \Delta) \rangle}{\partial B} \quad (2.31)$$

where the statistical average energy is calculated as:

$$\langle E(T, B, \omega_o, V_o, \Delta) \rangle = \frac{\sum_{\alpha=1}^N E_{\alpha} e^{-E_{\alpha}/k_B T}}{\sum_{\alpha=1}^N e^{-E_{\alpha}/k_B T}} \quad (2.32)$$

The aim of this work is to investigate the dependence of the magnetization of the double quantum dots on very rich and tunable parameters: the temperature ( $T$ ), magnetic field strength ( $\omega_c$ ), confining potential ( $\omega_0$ ), barrier height ( $V_o$ ) and barrier width ( $\Delta$ ).

## Chapter Three

### Result and Discussion

In this chapter we will present our computed results for two interacting electrons in double quantum dots made from GaAs material (*effective mass*  $m^* = 0.067 m_e$ , *effective Rydberg*  $R^* = 5.825 \text{ meV}$ ) confined by a parabolic potential of strength  $\omega_0$  under the effect of an applied uniform magnetic field of strength  $\omega_c$ , taken to be along z-direction, in addition to a Gaussian barrier of width  $\Delta$  and height  $V_0$ .

#### 3.1 DQD energy spectra:

As first essential step we have computed the eigenenergy spectra of DQD as function of magnetic field for specific values of confining frequency, barrier height and barrier width. Furthermore the exchange energy  $J$  is plotted as function of magnetic field strength, confining frequency, barrier height and barrier width. We compared the calculated energy spectra in Figure (3.1) and the exchange energy in Figure (3.4) with previous reported work [30]. The comparison obviously shows excellent agreement between both works.

We had plotted the computed energy results of this work against the strength of the magnetic field for  $\omega_0 = \frac{2}{3} R^*$ ,  $\Delta = 0.5 R^*$ ,  $V_0 = 1R^*$  for small range of  $\omega_c = \{0, 1R^*\}$  Figure (3.1) and large range of  $\omega_c = \{0, 4 R^*\}$  Figure (3.2), both figures shows the energy states with  $m = 0$ ,  $m = 1$  and  $m = 2$ . The numerical values of energy shown in Figure (3.1)

are also listed in Table 3.1. Figure (3.1) shows obviously the transition in the angular momentum of the ground state of the DQD system as the magnetic field strength increases. The origin of these transitions is due to the effect of coulomb interaction energy in the DQD Hamiltonian. The transitions in the angular momentum of the DQD system correspond to the (singlet-triplet) transitions are expected to manifest themselves as cusps in the magnetization curve of the DQD. The obtained results of the energy spectra and the exchange energy show very good agreement compared with Dyblaski's result [30]. Where the authors had used the variational method to solve the DQD Hamiltonian. In addition we had plotted the statistical energy against the strength of magnetic field in Figure (3.10) and Figure (3.11) to show the cusp in the energy- curve that causes the cusps in the magnetization-curve of the DQD.

Moreover, we have calculated the exchange energy  $J$  of SQD and DQD. In Figure (3.4) we have displayed the exchange energy  $J$  of DQD as a function of field strength for  $\omega_0 = \frac{2}{3} R^*$ ,  $\Delta = 0.5 R^*$ ,  $V_o = 1R^*$ .

In Figure (3.5) we have sketched our computed results for the exchange energy  $J$  against the magnetic field strength for SQD. In addition we have sketched our computed results for the exchange energy  $J$  against the magnetic field strength for SQD and DQD jointly in Figure (3.6) for comparison purpose. We noticed that the  $J$ -curve for SQD shows a large and sharp minimum value while the corresponding  $J$ -curve for DQD shows a small and smooth minimum behavior.

In Figure (3.7) we have investigated the effect of barrier height on the exchange energy, it is obvious from the figure that as  $V_o$  increases the minimum of the exchange energy curve shifts to lower magnetic field strength.

The effect of confining frequency  $\omega_0$  is also very important on the exchange energy quantity. As shown in Figure (3.8), as  $\omega_0$  increases the minimum of the exchange energy curve shifts to higher magnetic field strength.

We have also examined the phase diagrams of the exchange energy curve for DQD system. In Figure 3.9 (a) we have shown the phase diagrams of  $\omega_c$  against  $\omega_0$  for DQD for  $V_o = 1$  when  $J = 0$ , the plot shows a linear relationship between  $\omega_c$  and  $\omega_0$ . In Figure 3.9 (b) we have shown the phase diagrams of  $\omega_c$  against  $V_o$  for DQD for  $\omega_0 = \frac{2}{3}$  when  $J = 0$ , the plot shows a linear relationship between  $\omega_c$  and  $V_o$ .

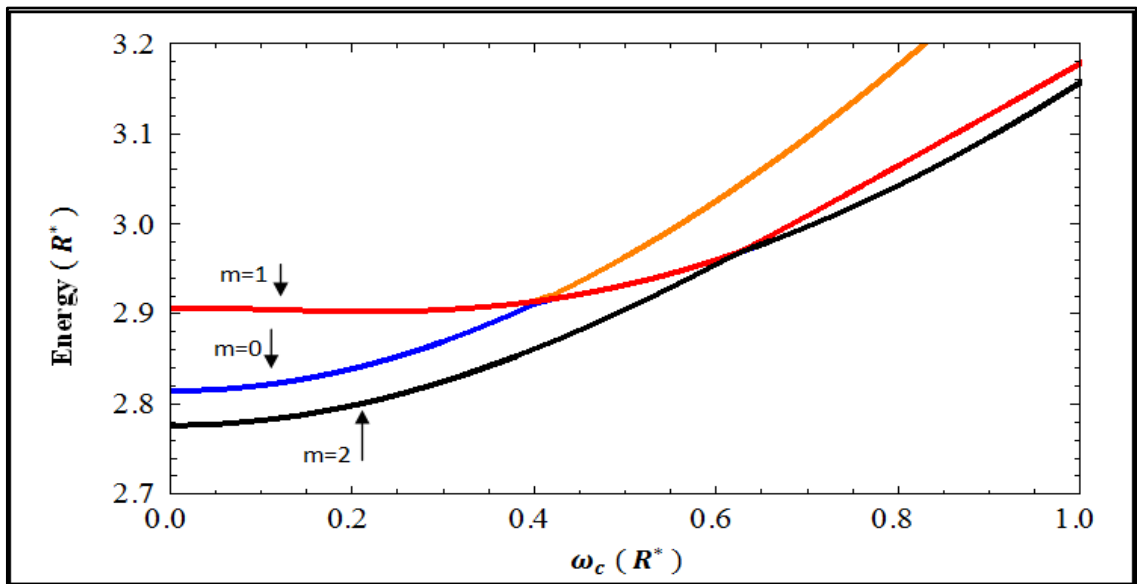


**Figure (3.1): a) The computed energy spectra of two interacting electrons in double quantum dots against the strength of the magnetic field.**

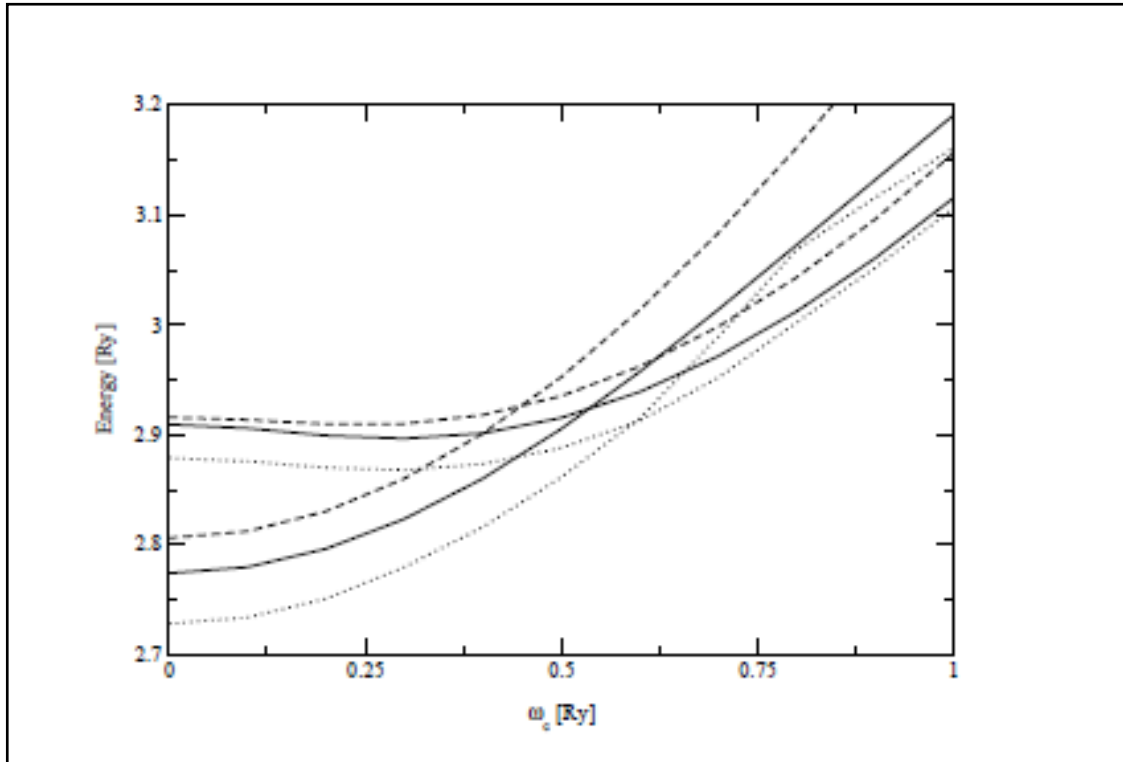


Figure (3.1): b) The computed energy spectra of two interacting electrons in double quantum dots against the strength of the magnetic field for the range of  $\omega_c = \{0, 4R^*\}$ , and angular momentum  $m = 0, 1, 2$ .

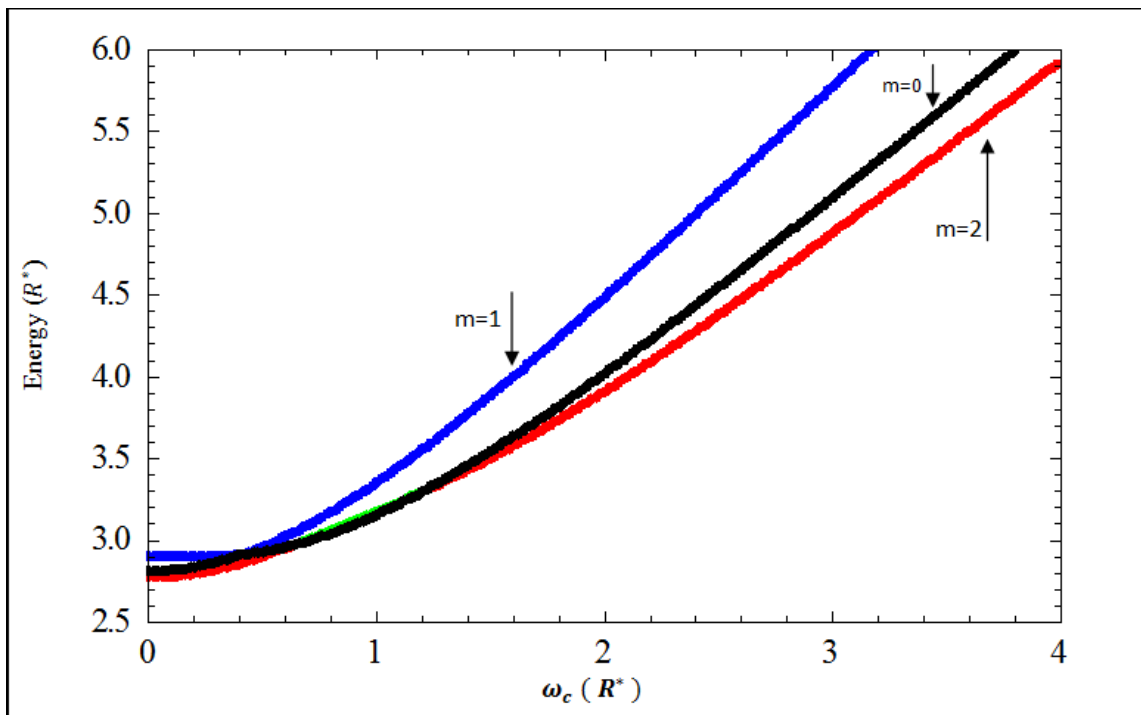


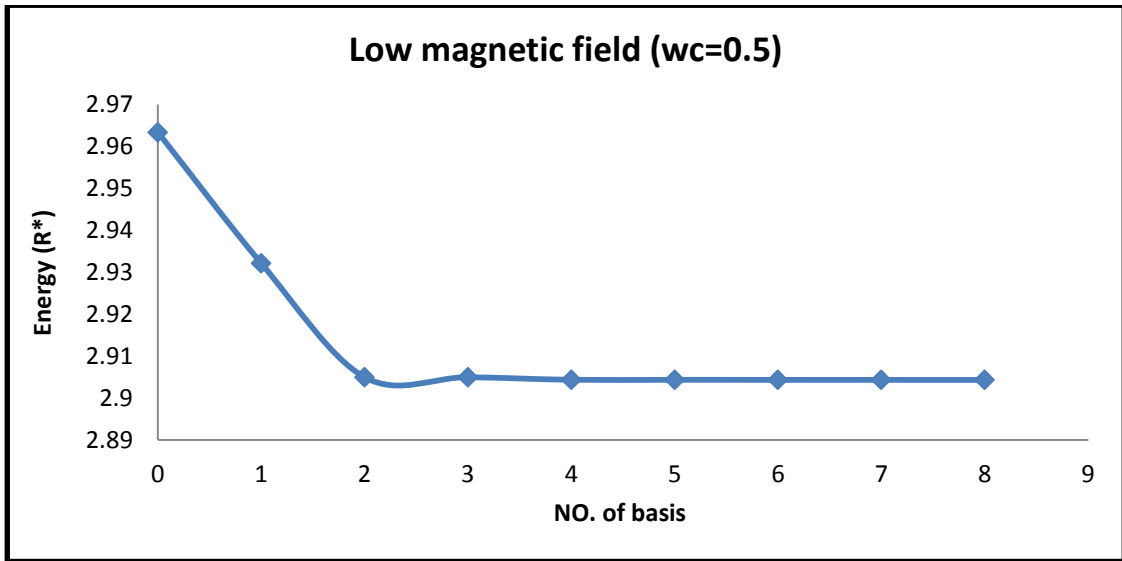
Figure (3.2): The computed energy spectra of two interacting electrons in double quantum dots against the strength of the magnetic field.

**Table (3.1):** Our computed energy spectra of the DQD states against the magnetic field for two interacting electrons for  $\omega_o = \frac{2}{3} R^*$ ,  $\Delta = 0.5 R^*$ ,  $V_o = 1R^*$ .

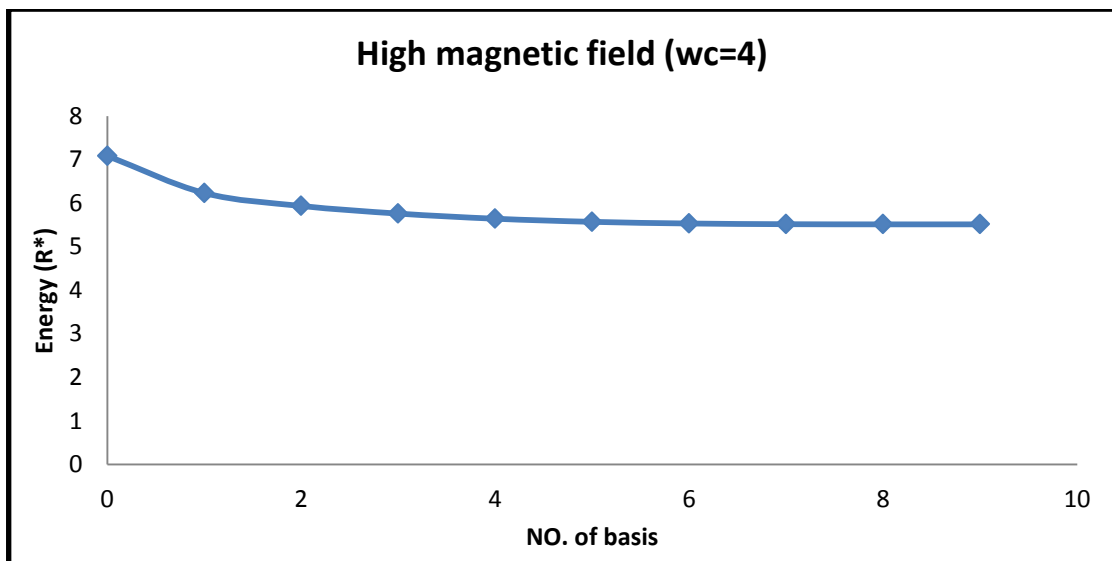
$\omega_c(R^*)$	Energies in $R^*$ for DQD				
0.	3.59493	3.45741	3.18594	2.90677	2.77626
0.02	3.598	3.45507	3.1866	2.90669	2.77648
0.04	3.60665	3.44859	3.18855	2.90648	2.77715
0.06	3.61967	3.43919	3.19178	2.90613	2.77826
0.08	3.63587	3.42805	3.19626	2.90567	2.77981
0.1	3.65442	3.41602	3.20196	2.90515	2.78179
0.12	3.67476	3.40364	3.20884	2.90459	2.78422
0.14	3.69653	3.39125	3.21685	2.90404	2.78708
0.16	3.71952	3.37908	3.22595	2.90354	2.79037
0.18	3.74357	3.36727	3.23608	2.90313	2.79408
0.2	3.76859	3.35592	3.2472	2.90285	2.79821
0.22	3.79451	3.34508	3.25926	2.90274	2.80276
0.24	3.82126	3.33481	3.27223	2.90283	2.80771
0.26	3.84882	3.32513	3.28605	2.90316	2.81306
0.28	3.87715	3.31607	3.3007	2.90374	2.8188
0.3	3.90622	3.31614	3.30765	2.90461	2.82493
0.32	3.93602	3.33233	3.29987	2.90579	2.83143
0.34	3.96652	3.34926	3.29275	2.90728	2.8383
0.36	3.99771	3.36689	3.2863	2.90911	2.84552
0.38	4.02958	3.3852	3.28051	2.91129	2.85308
0.4	4.0621	3.40416	3.27541	2.91383	2.86098
0.42	4.09527	3.42375	3.27098	2.91674	2.86919
0.44	4.12908	3.44396	3.26723	2.92001	2.87771
0.46	4.1635	3.46476	3.26416	2.92367	2.88652
0.48	4.19854	3.48614	3.26178	2.9277	2.8956
0.5	4.23417	3.50808	3.2601	2.93211	2.90495

Continued Table (3.1)

$\omega_c(R^*)$	Energies in $R^*$ for DQD				
0.52	4.2704	3.53057	3.2591	2.9369	2.91454
0.54	4.3072	3.55358	3.2588	2.94208	2.92436
0.56	4.34456	3.57711	3.2592	2.94763	2.93439
0.58	4.38248	3.60115	3.26029	2.95356	2.94461
0.6	4.42095	3.62567	3.2621	2.95986	2.955
0.62	4.45994	3.65067	3.2646	2.96654	2.96556
0.64	4.49947	3.67614	3.26782	2.97625	2.97358
0.66	4.5395	3.70205	3.27175	2.98706	2.98099
0.68	4.58004	3.72841	3.27639	2.99797	2.98875
0.7	4.62107	3.7552	3.28175	3.00897	2.99687
0.72	4.66258	3.78241	3.28782	3.02003	3.00534
0.74	4.70456	3.81002	3.29461	3.03116	3.01415
0.76	4.74701	3.83804	3.3021	3.04232	3.0233
0.78	4.78991	3.86644	3.3103	3.05352	3.03278
0.8	4.83325	3.89522	3.31919	3.06474	3.04258
0.82	4.87702	3.92437	3.32877	3.07599	3.05271
0.84	4.92122	3.95388	3.33903	3.08724	3.06314
0.86	4.96583	3.98374	3.34994	3.09851	3.07389
0.88	5.01084	4.01394	3.3615	3.10979	3.08494
0.9	5.05625	4.04447	3.37369	3.1211	3.09628
0.92	5.10205	4.07533	3.38648	3.13242	3.10791
0.94	5.14823	4.10651	3.39985	3.14378	3.11983
0.96	5.19477	4.13799	3.41379	3.15517	3.13202
0.98	5.24168	4.16977	3.42826	3.16661	3.14449
1.	5.28894	4.20185	3.44325	3.17811	3.15722



a)



b)

**Figure (3.3):** The energy of DQD for fixed values of  $\omega_0 = \frac{2}{3}R^*$ ,  $\Delta = 0.5 R^*$ ,  $V_o = 1R^*$  against the number of basis and various confining cyclotron frequencies, a) at  $\omega_c = 0.5R^*$  and b) at  $\omega_c = 4R^*$ .

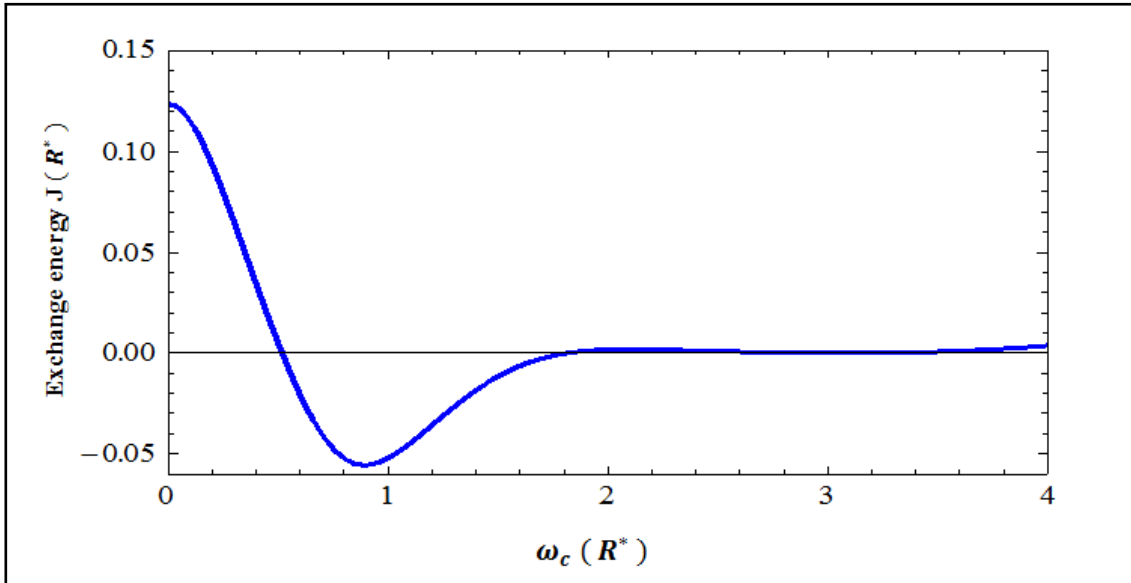


Figure (3.4): a) Our computed exchange energy of the two interacting electrons in DQD against the magnetic field strength for  $\omega_o = \frac{2}{3} R^*$ ,  $\Delta = 0.5 R^*$ ,  $V_o = 1 R^*$ .

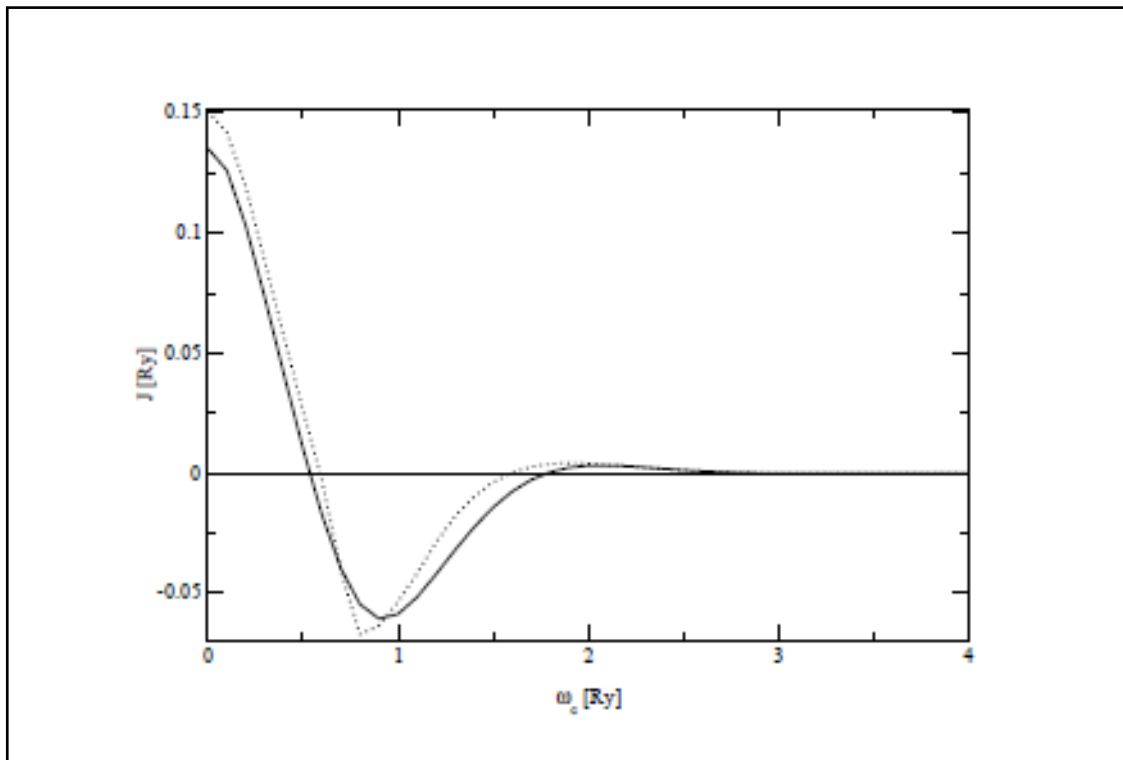


Figure (3.4): b) The computed exchange energy of the two interacting electrons in DQD against the magnetic field strength in Ref [30].

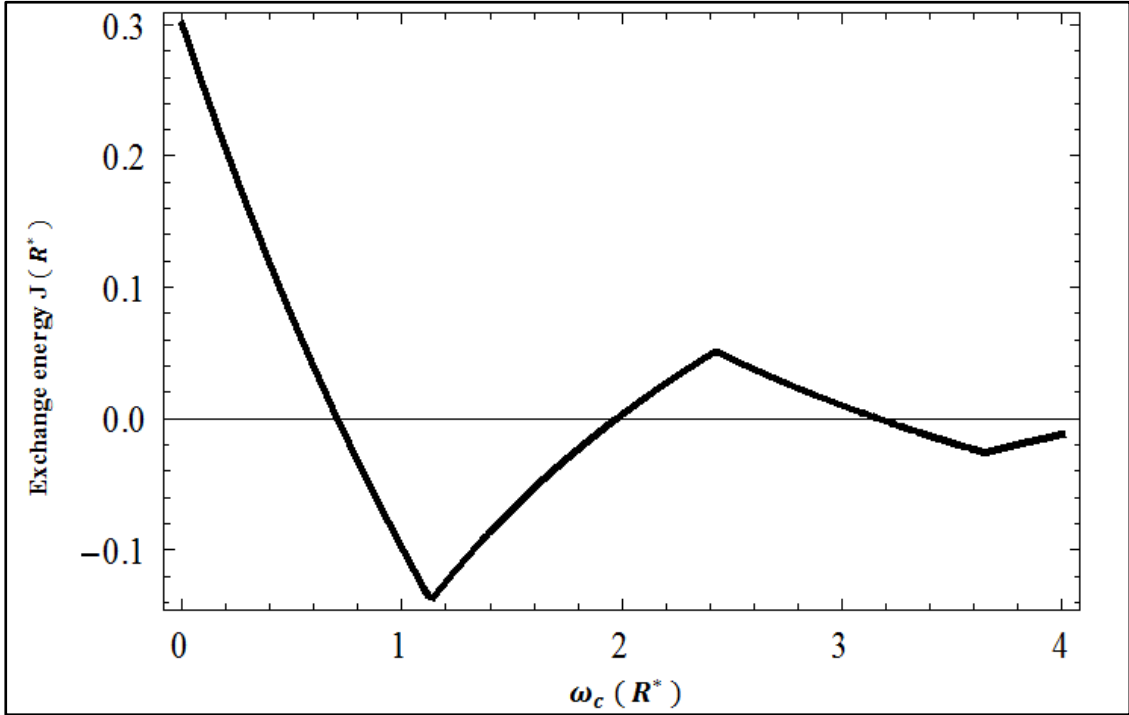


Figure (3.5): The exchange energy of the two interacting electrons in SQD against the magnetic field strength for  $\omega_o = \frac{2}{3} R^*$  results by turning off the  $V_b$  - term in the DQD Hamiltonian.

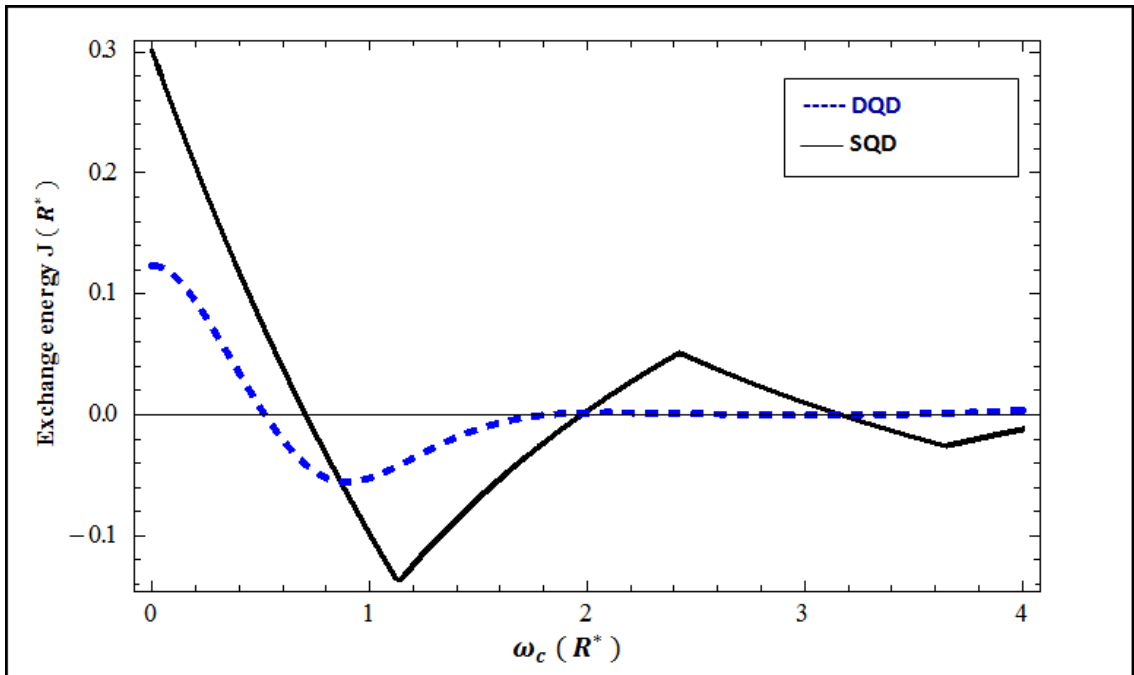


Figure (3.6): Comparison between the exchange energy of the two interacting electrons in SQD for  $\omega_o = \frac{2}{3} R^*$  results by turning off the  $V_b$  - term in the DQD Hamiltonian (solid curve), and the exchange energy of the two interacting electrons in DQD for  $\omega_o = \frac{2}{3} R^*$ ,  $\Delta = 0.5 R^*$ ,  $V_o = 1 R^*$  against the magnetic field strength (dashed curve).

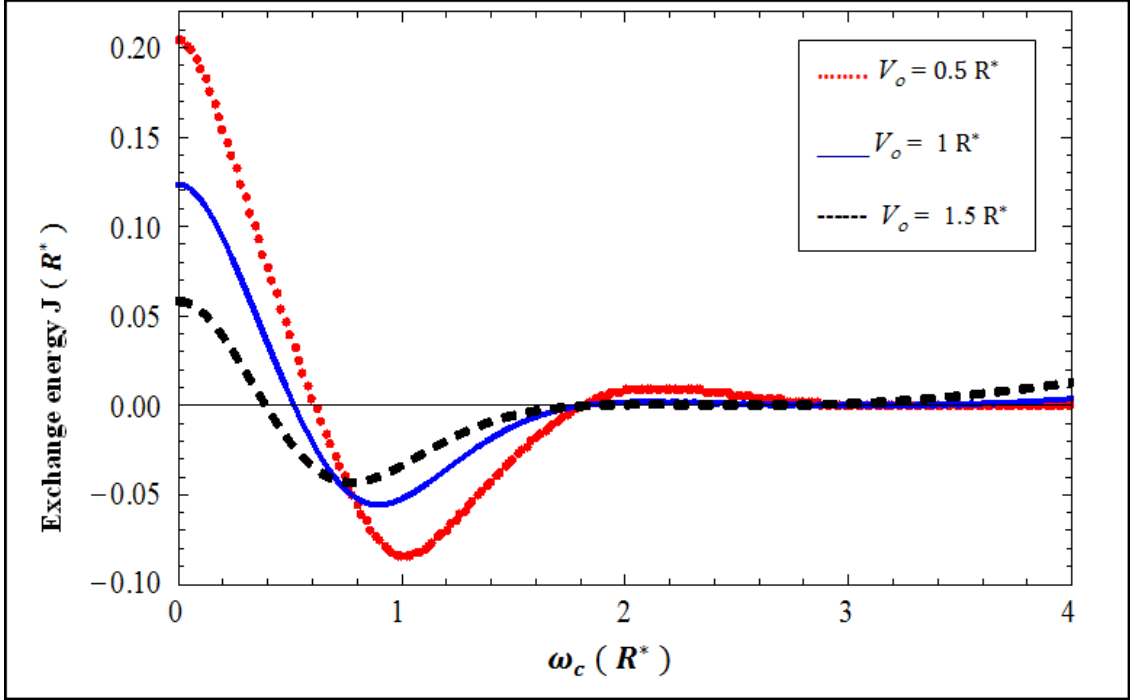


Figure (3.7): The exchange energy of the two interacting electrons in DQD against the magnetic field strength for  $\omega_o = \frac{2}{3} R^*$ ,  $\Delta = 0.5 R^*$  and different values of  $V_o$ , the (dotted curve) at  $V_o = 0.5 R^*$ , the (solid curve) at  $V_o = 1 R^*$  and (the dashed curve) at  $V_o = 1.5 R^*$ .

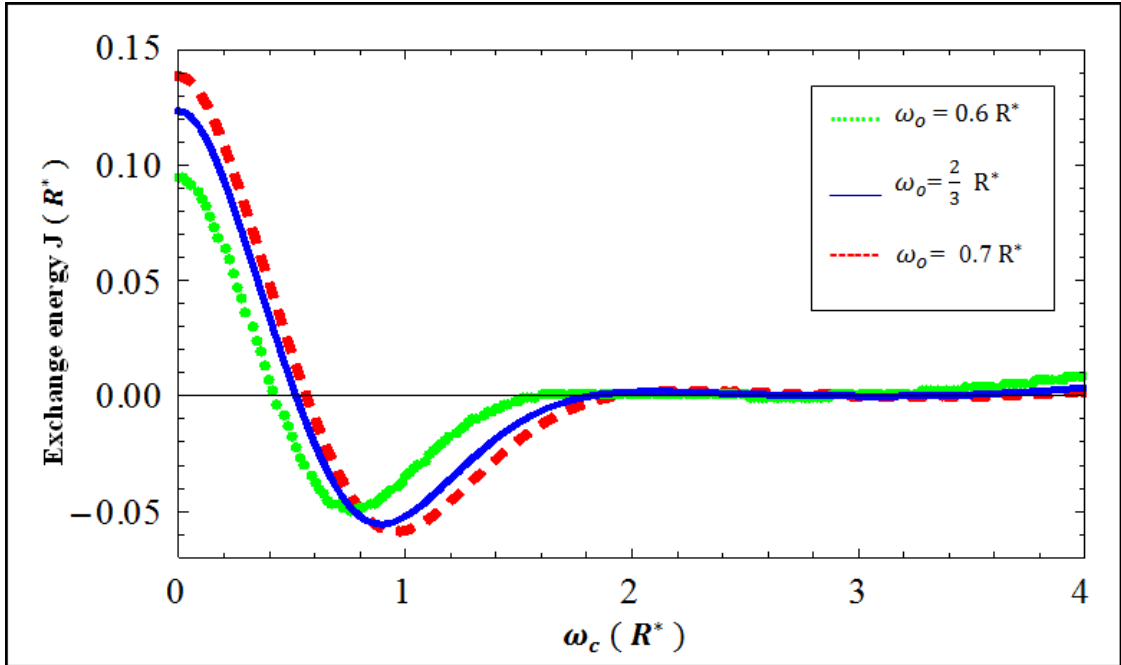
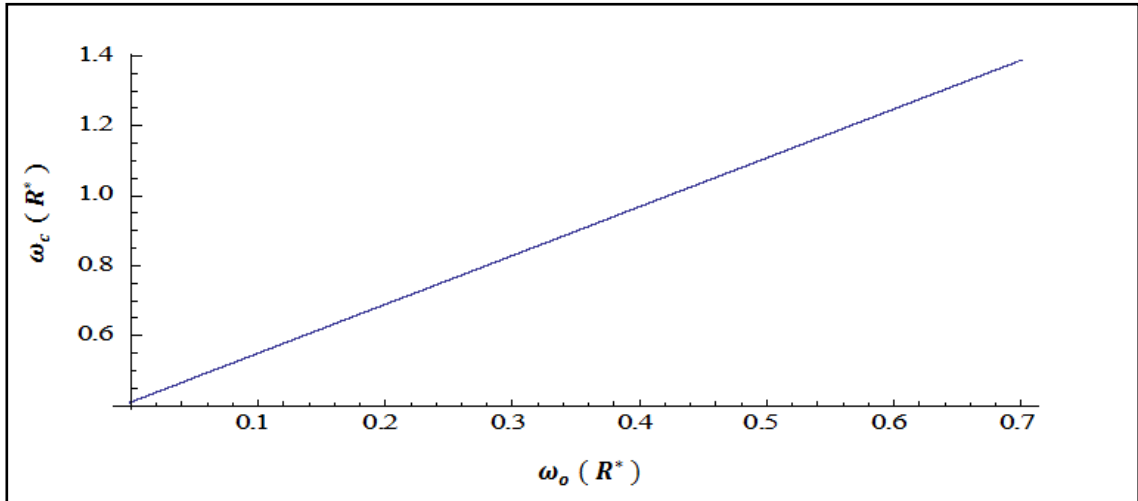
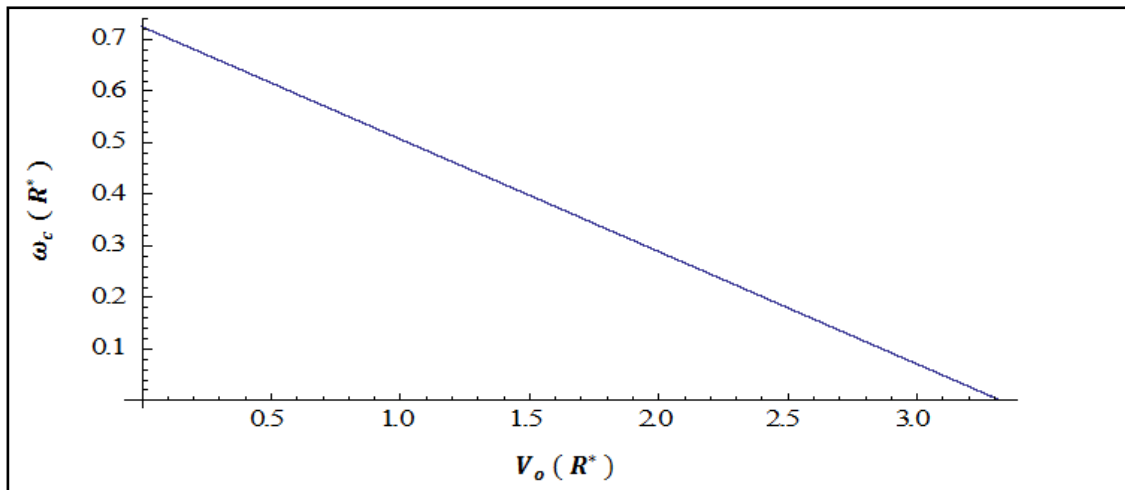


Figure (3.8): The exchange energy of the two interacting electrons in DQD against the magnetic field strength for  $V_o = 1 R^*$ ,  $\Delta = 0.5 R^*$  and different values of  $\omega_o$ , the (dashed curve) at  $\omega_o = 0.7 R^*$ , the (solid curve) at  $\omega_o = \frac{2}{3} R^*$  and the (dotted curve) at  $\omega_o = 0.6 R^*$ .



a)



b)

**Figure (3.9):** Phase diagrams for the exchange energy, a) The relation between  $\omega_c (R^*)$  and  $\omega_0 (R^*)$  at  $V_o = 1 R^*$ .

b) The relation between  $\omega_c (R^*)$  and  $V_o (R^*)$  at  $\omega_0 = \frac{2}{3} R^*$ .

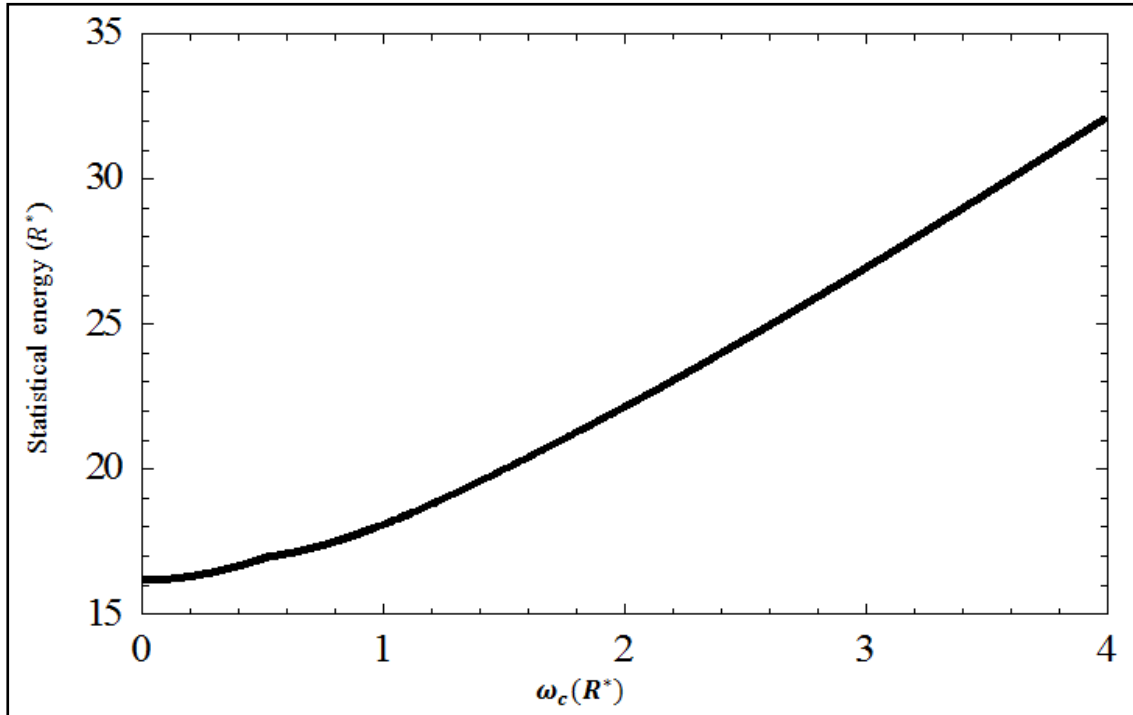


Figure (3.10): The statistical energy of two interacting electrons in double quantum dots against the strength of the magnetic field for  $\omega_0 = \frac{2}{3} R^*$ ,  $\Delta = 0.5 R^*$ ,  $V_o = 1 R^*$ .

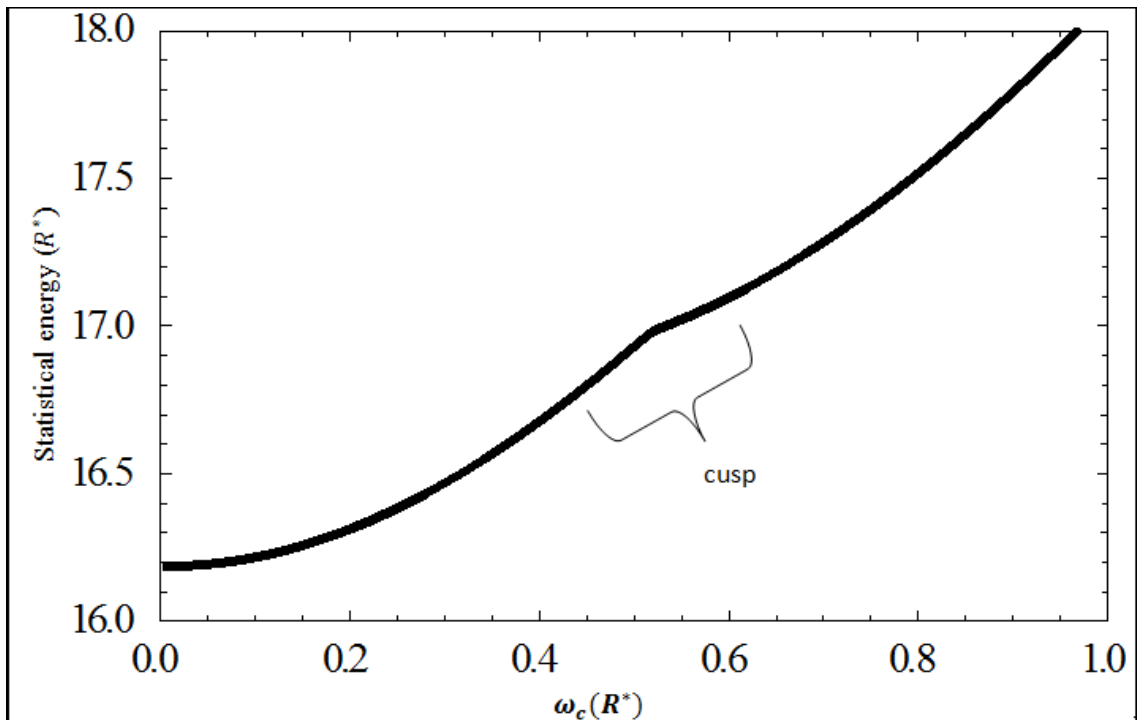


Figure (3.11): The statistical energy of two interacting electrons in double quantum dots against the strength of the magnetic field for  $\omega_0 = \frac{2}{3} R^*$ ,  $\Delta = 0.5 R^*$ ,  $V_o = 1 R^*$ . The curve shows a cusp at  $\omega_c = 0.5 R^*$ .

### 3.2 Magnetization:

The second step in our work is the calculation of the magnetization of DQD as a function of various QD parameters  $\omega_0, \Delta, V_o, \omega_c, T$ .

In Figure (3.12), we have computed magnetization curve for DQD against the magnetic field strength. The curve clearly shows the cusps which are attributed to the effect of electron-electron interaction in the DQD Hamiltonian. Moreover we have presented the same magnetization plot for SQD in Figure (3.13). We have compared both magnetization behaviors for SQD and DQD systems in Figure (3.14). This figure shows that the magnetization curve of SQD has negative and positive values, while the magnetization curve of DQD has only negative values.

We have also plotted in Figure (3.15) the magnetization of DQD system as function of the magnetic field strength at three different temperatures Figure 3.15 (a, b and c) and show the curves in the same plot Figure 3.15 (d) to compare between them. We noticed from the figure that there are differences at the cusps of the magnetization curves. Moreover we have investigated the differences by focusing on the cusps of the three curves in Figure (3.16) and Figure (3.17). We have noticed from the figures that the heights of the peaks due to transition jumps are reduced, broadened and shifted to higher magnetic value as the temperature increased.

In addition we have investigated the effect of the barrier height on the magnetization curve. For this purpose we have plotted the

magnetization curve at different barrier heights independently in Figure 3.18 (a, b and c) and compare between them at the same graph in Figure 3.18 (d). The Figure 3.18 (d) clearly shows the gradual shift of the magnetization jumps to higher magnetic field as the barrier height decreases.

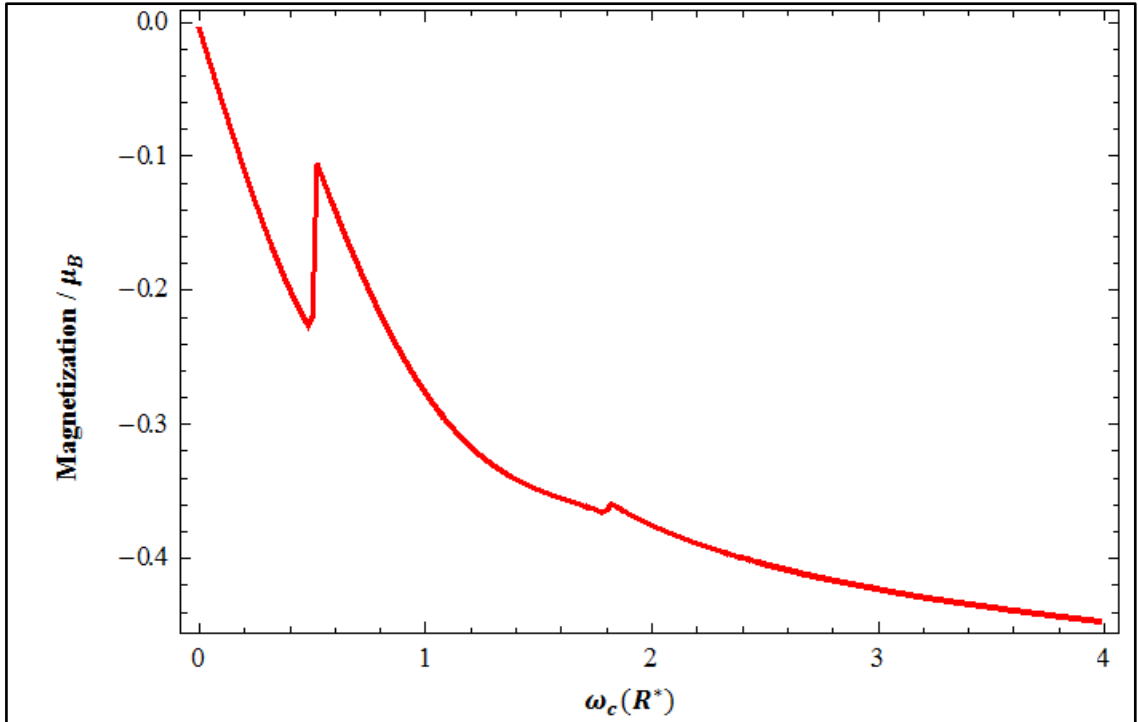


**Figure (3.12):** The magnetization (in unit of  $\mu_B = \frac{e\hbar}{2m^*} = 0.87 \text{ meV/T}$  for GaAs) at  $T = 0.01 \text{ K}$ , of the two interacting electrons in DQD against the magnetic field strength for  $\omega_o = \frac{2}{3} R^*$ ,  $\Delta = 0.5 R^*$ ,  $V_o = 1 R^*$ .

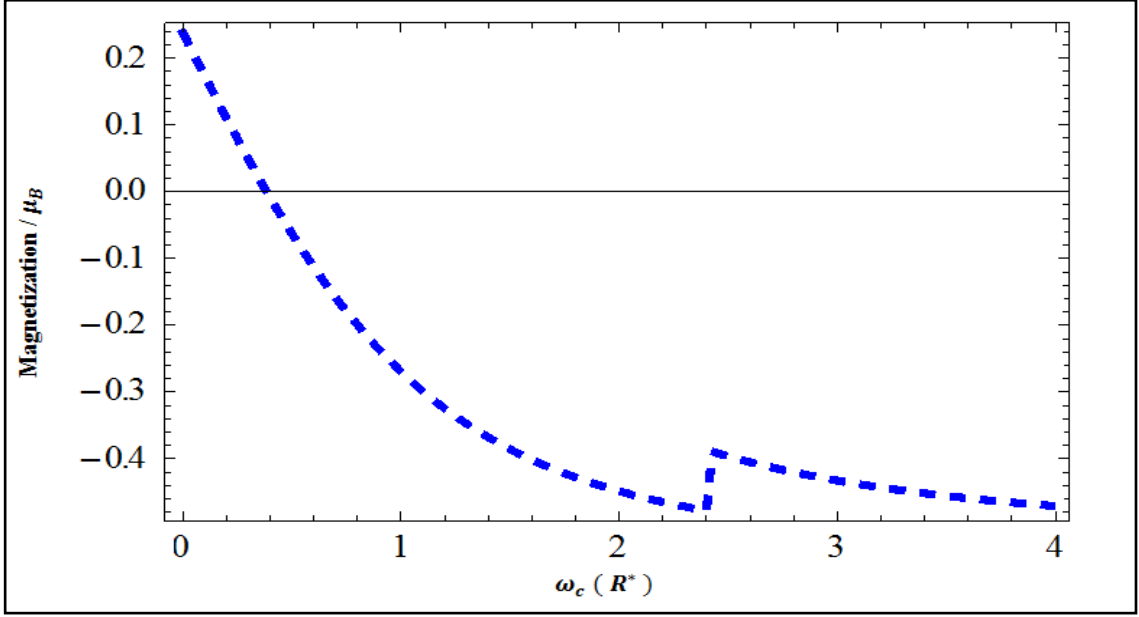


Figure (3.13): The magnetization (in unit of  $\mu_B = \frac{e\hbar}{2m^*} = 0.87 \text{ meV/T}$  for GaAs) at  $T = 0.01 \text{ K}$ , of the two interacting electrons in SQD against the magnetic field strength for  $\omega_o = \frac{2}{3} R^*$  results by turning off the  $V_b$ - term in the DQD Hamiltonian.

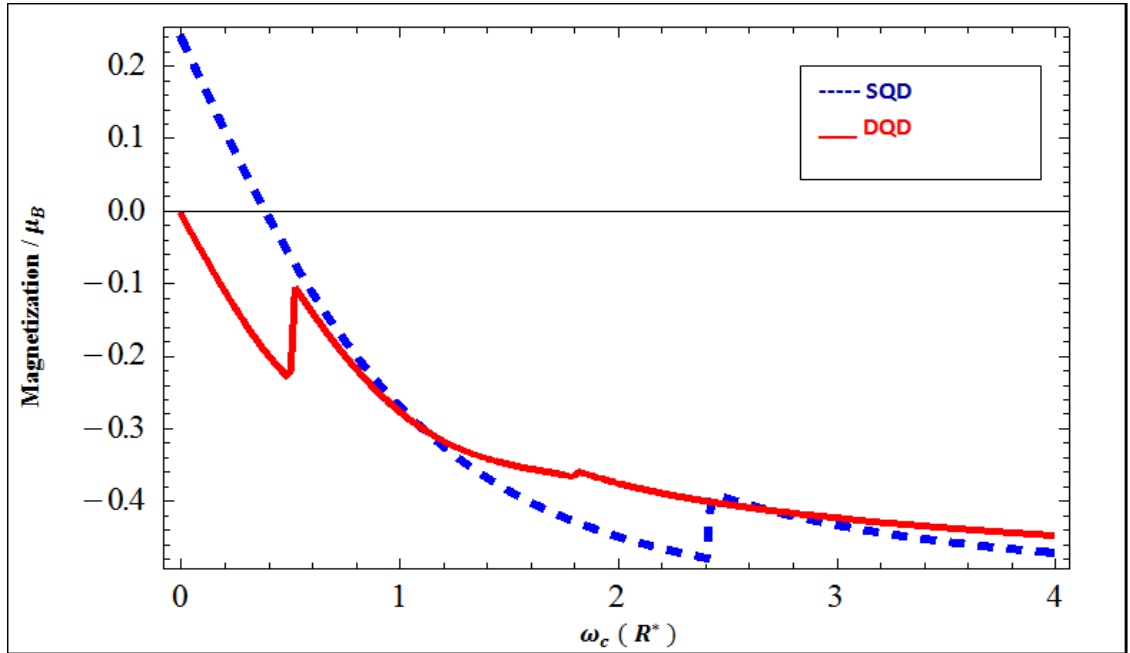


Figure (3.14): Comparison between the magnetization (in unit of  $\mu_B$ ) at  $T = 0.01 \text{ K}$  of the two interacting electrons in SQD (dashed curve) for  $\omega_o = \frac{2}{3} R^*$  results by turning off the  $V_b$ - term in the DQD Hamiltonian, and the magnetization (in unit of  $\mu_B$ ) at  $T = 0.01 \text{ K}$  of the two interacting electrons in DQD (solid curve) for  $\omega_o = \frac{2}{3} R^*$ ,  $\Delta = 0.5 R^*$ ,  $V_o = 1 R^*$  against the magnetic field strength.

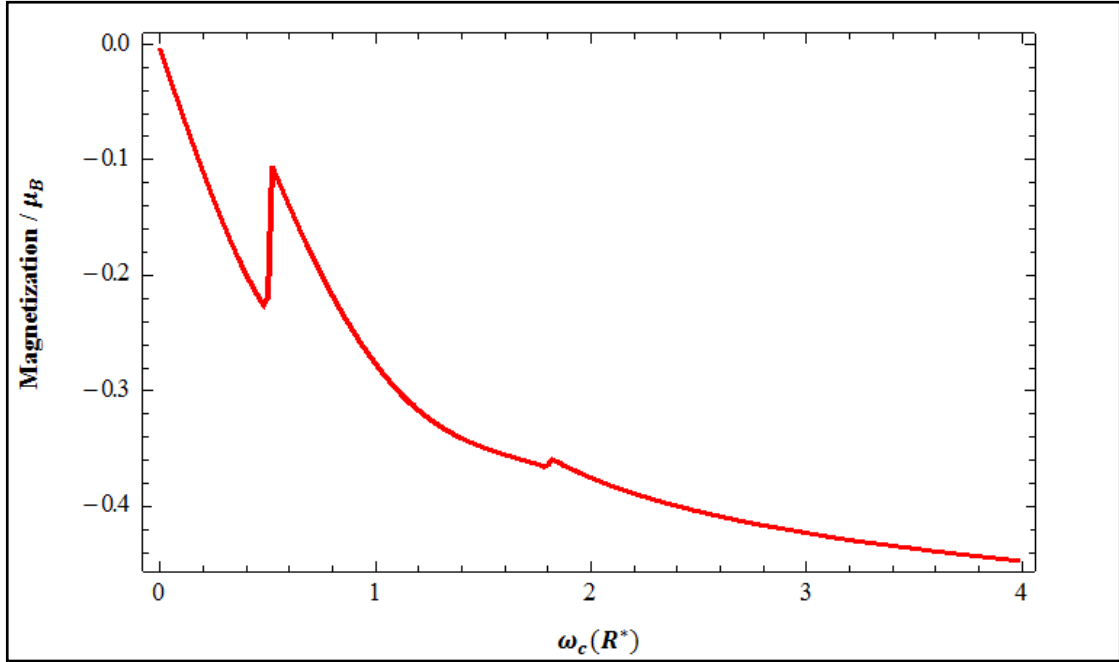


Figure (3.15): a) The magnetization (in unit of  $\mu_B = \frac{e\hbar}{2m^*} = 0.87 \text{ meV/T}$  for GaAs) of the two interacting electrons in DQD against the magnetic field strength for  $\omega_o = \frac{2}{3} R^*$ ,  $\Delta = 0.5 R^*$ ,  $V_o = 1R^*$  at  $T = 0.01 \text{ K}$ .

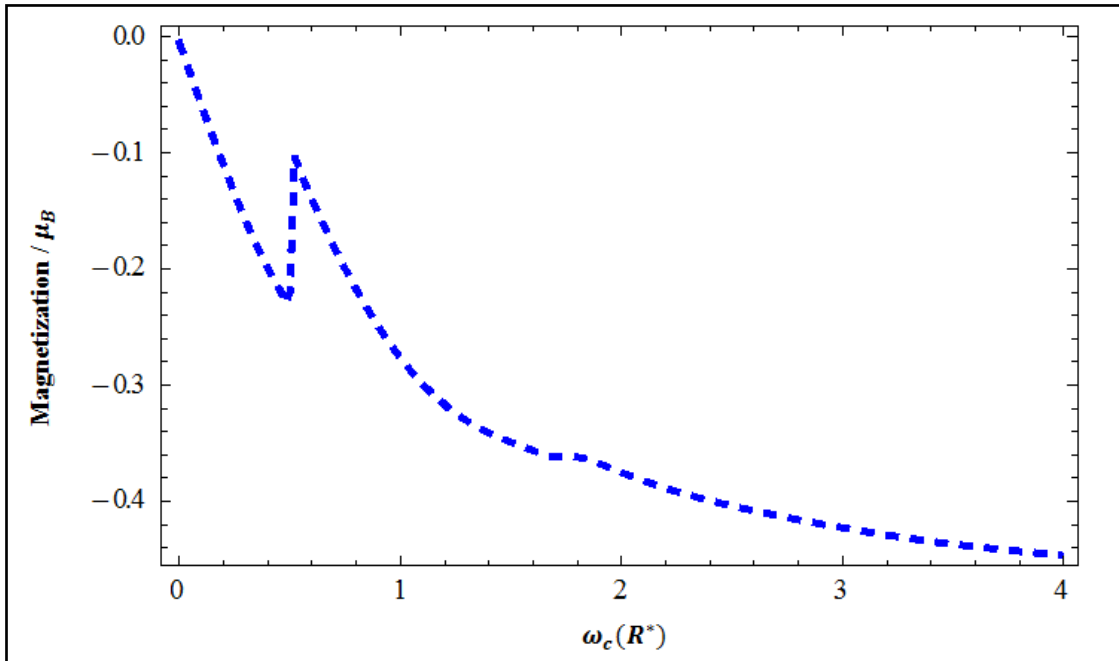


Figure (3.15): b) Same as Figure 3.15 (a) but at  $T = 0.1 \text{ K}$ .

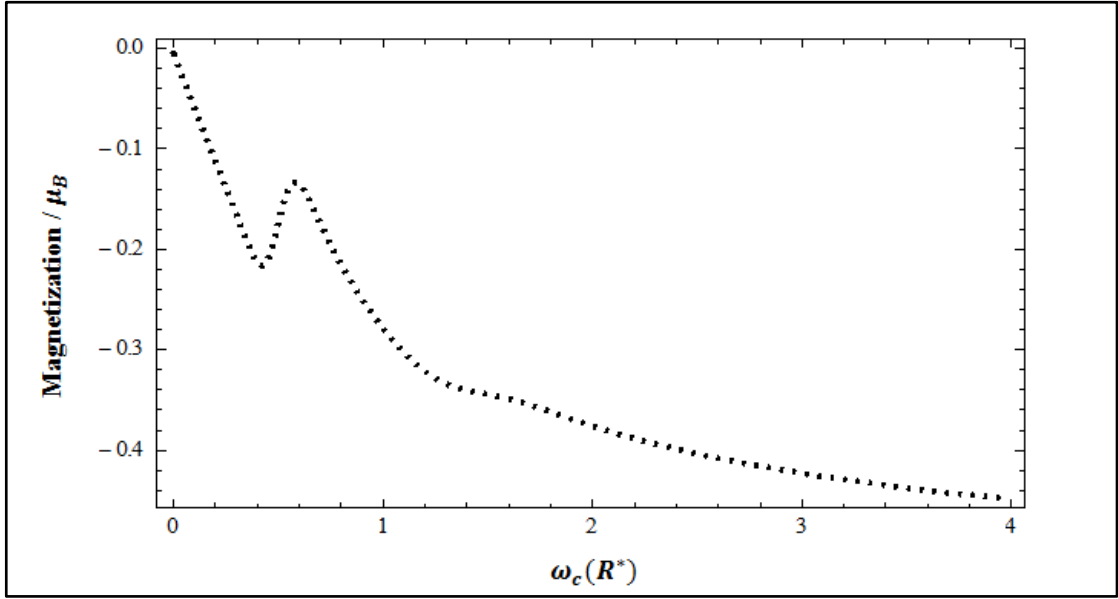


Figure (3.15): c) Same as Figure 3.15 (a) but at at T = 1 K.

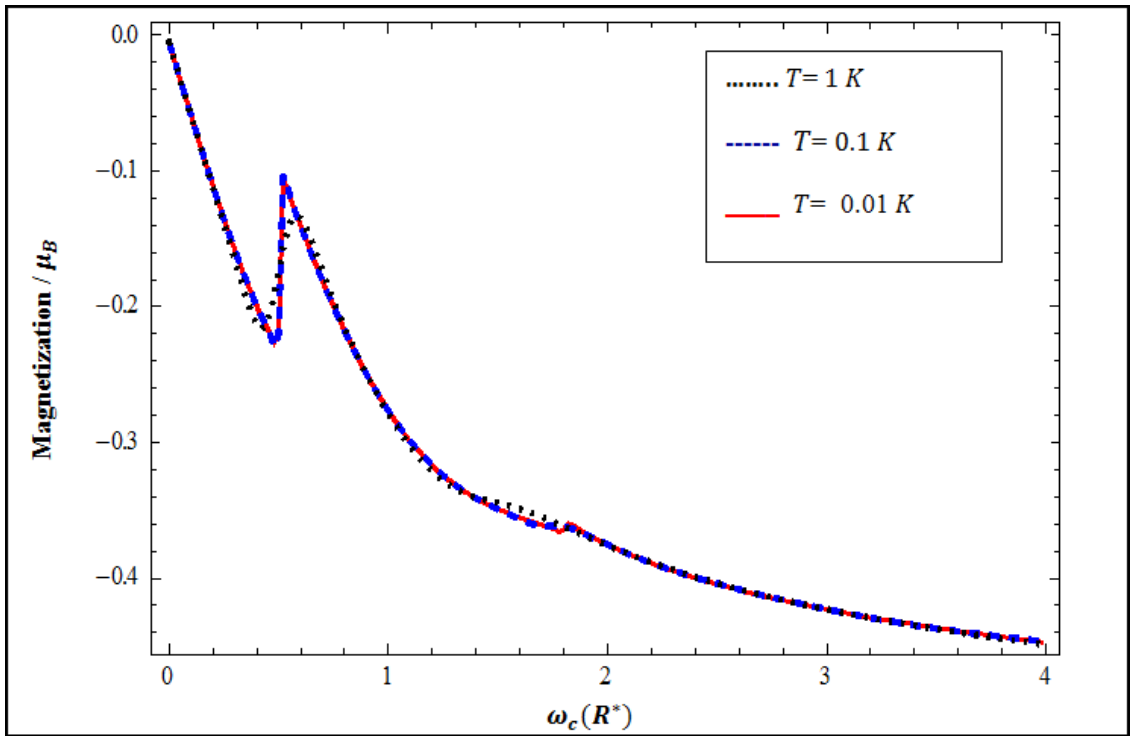


Figure (3.15): d) The magnetization (in unit of  $\mu_B = \frac{e\hbar}{2m^*} = 0.87 \text{ meV/T}$  for GaAs) of the two interacting electrons in DQD against the magnetic field strength for  $\omega_o = \frac{2}{3} R^*$ ,  $\Delta = 0.5 R^*$ ,  $V_o = 1R^*$  at different temperatures. a) The (solid curve) at 0.01 K, b) the (dashed curve) at 0.1 K and c) the (dotted curve) at 1 K.

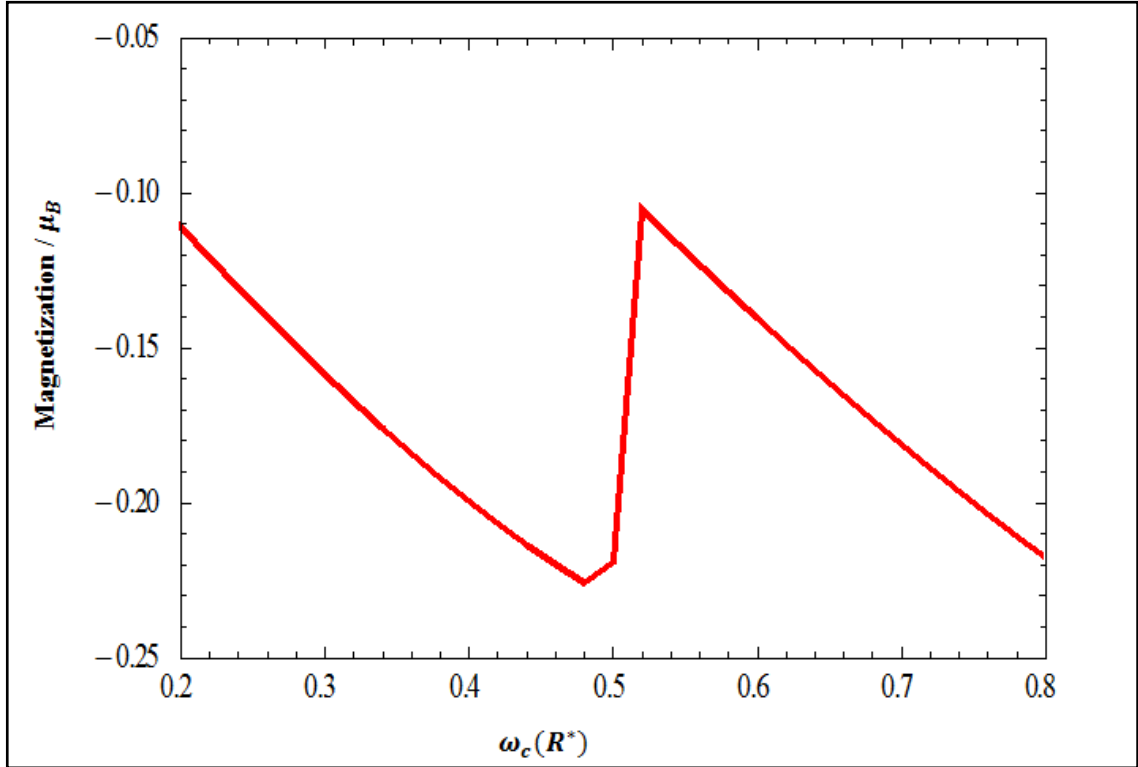


Figure (3.16): a) The magnetization (in unit of  $\mu_B = \frac{e\hbar}{2m^*} = 0.87 \text{ meV/T}$  for GaAs) of the two interacting electrons in DQD against the magnetic field strength showing the first cusp, for  $\omega_o = \frac{2}{3} R^*$ ,  $\Delta = 0.5 R^*$ ,  $V_o = 1R^*$  at  $T = 0.01 \text{ K}$ .

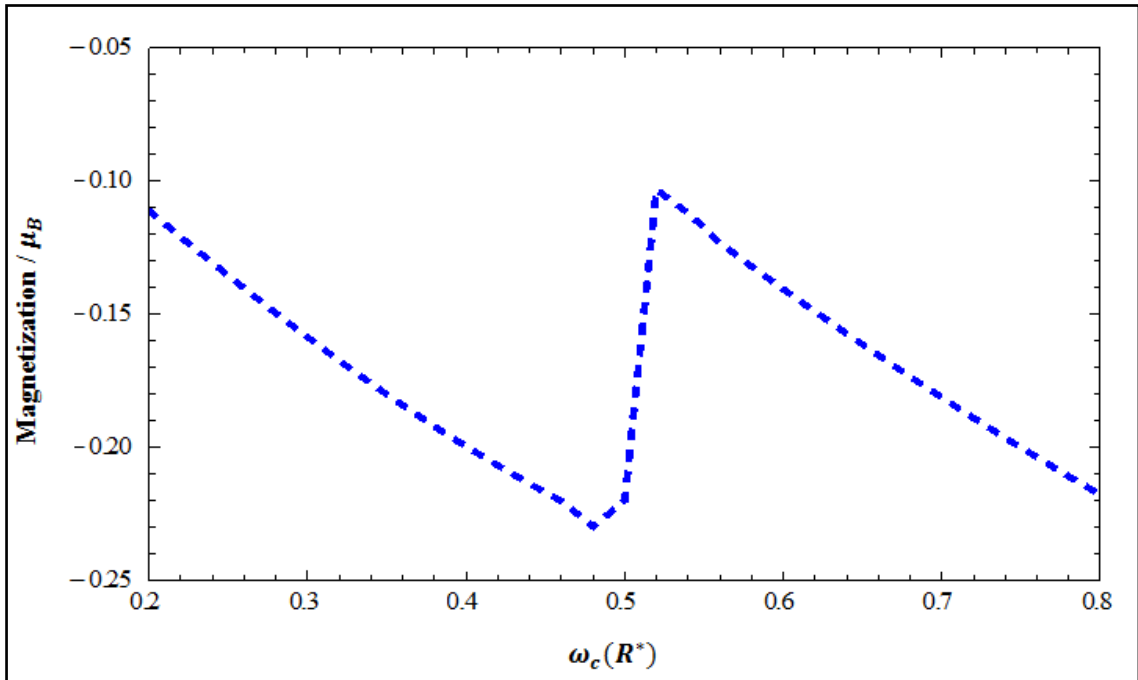


Figure (3.16): b) Same as Figure 3.16 (a) but at  $T = 0.1 \text{ K}$ .

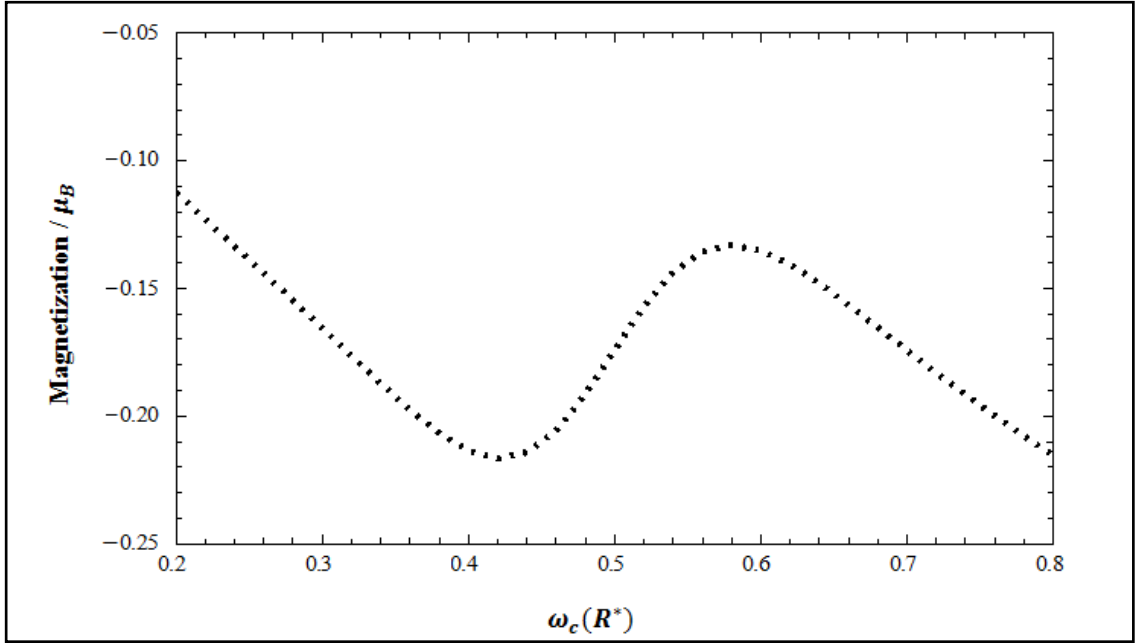


Figure (3.16): c) Same as Figure 3.16 (a) but at  $T = 1$  K.

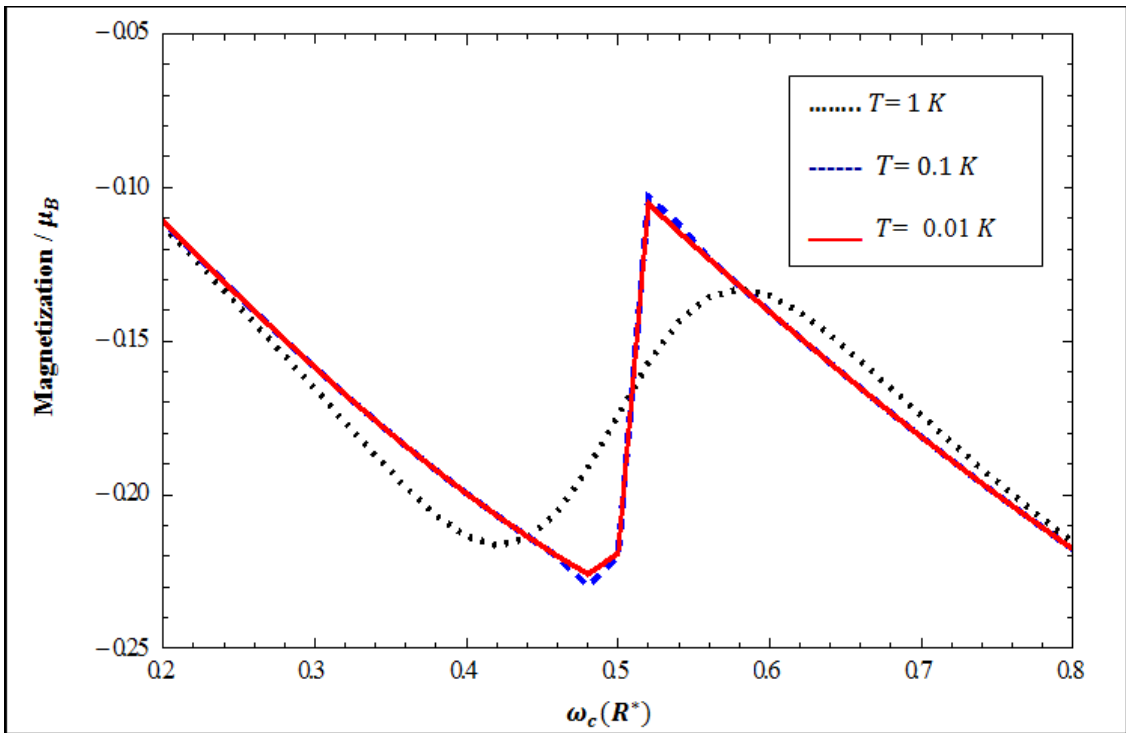


Figure (3.16): d) The magnetization (in unit of  $\mu_B = \frac{e\hbar}{2m^*} = 0.87 \text{ meV/T}$  for GaAs) of the two interacting electrons in DQD against the magnetic field strength showing the first cusp for  $\omega_o = \frac{2}{3} R^*$ ,  $\Delta = 0.5 R^*$ ,  $V_o = 1 R^*$  at different temperatures. a) The (solid curve) at 0.01 K, b) the (dashed curve) at 0.1 K and c) the (dotted curve) at 1K.

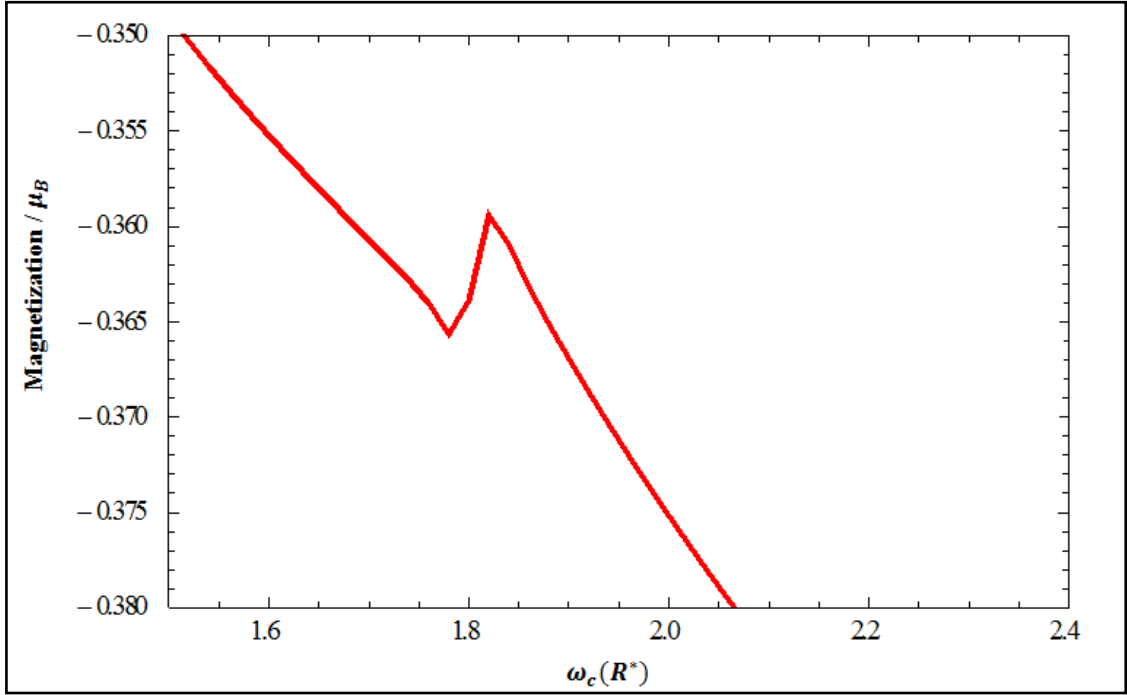


Figure (3.17): a) The magnetization (in unit of  $\mu_B = \frac{e\hbar}{2m^*} = 0.87 \text{ meV/T}$  for GaAs) of the two interacting electrons in DQD against the magnetic field strength showing the second cusp, for  $\omega_o = \frac{2}{3} R^*$ ,  $\Delta = 0.5 R^*$ ,  $V_o = 1R^*$  at  $T = 0.01 \text{ K}$ .

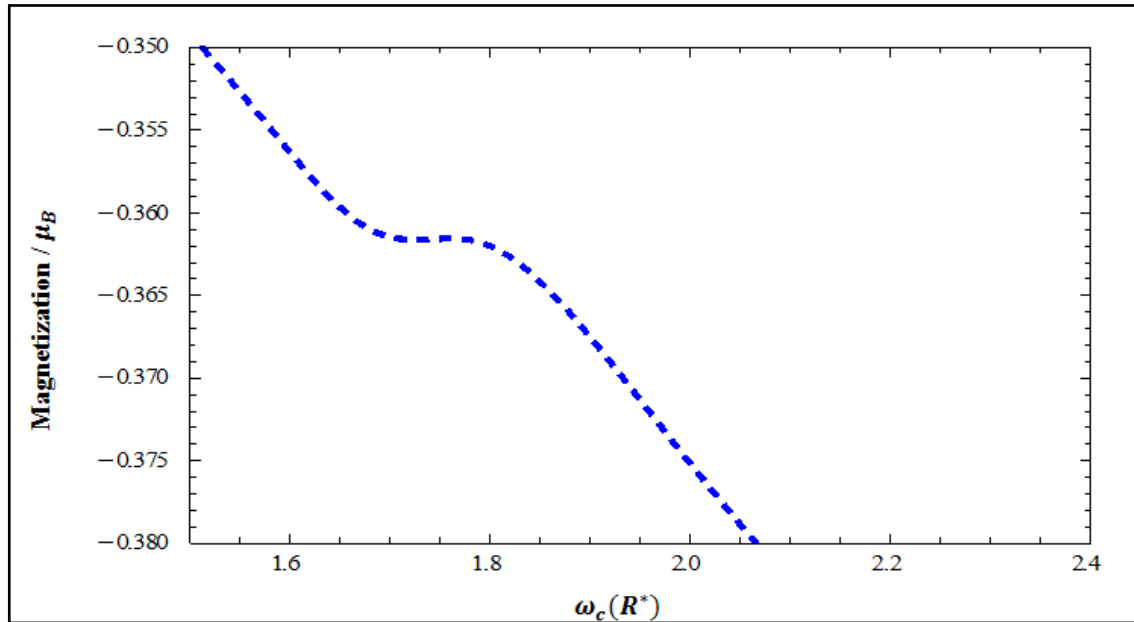


Figure (3.17): b) Same as Figure 3.17 (a) but at  $T = 0.1 \text{ K}$ .

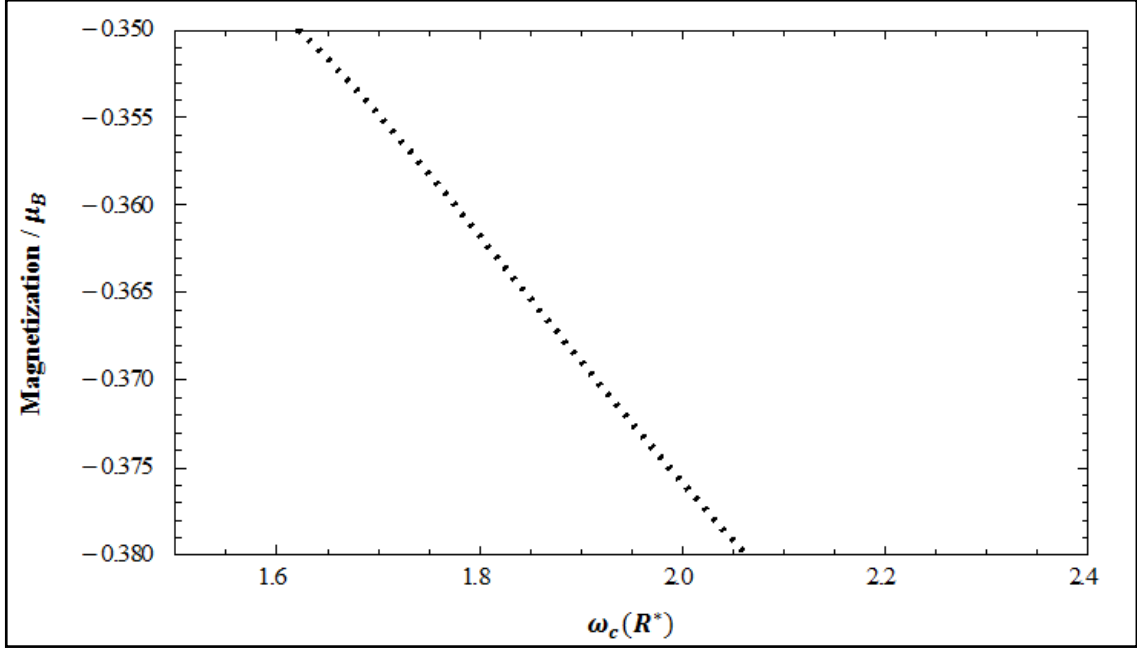


Figure (3.17): c) Same as Figure 3.17 (a) but at  $T = 1\text{K}$ .

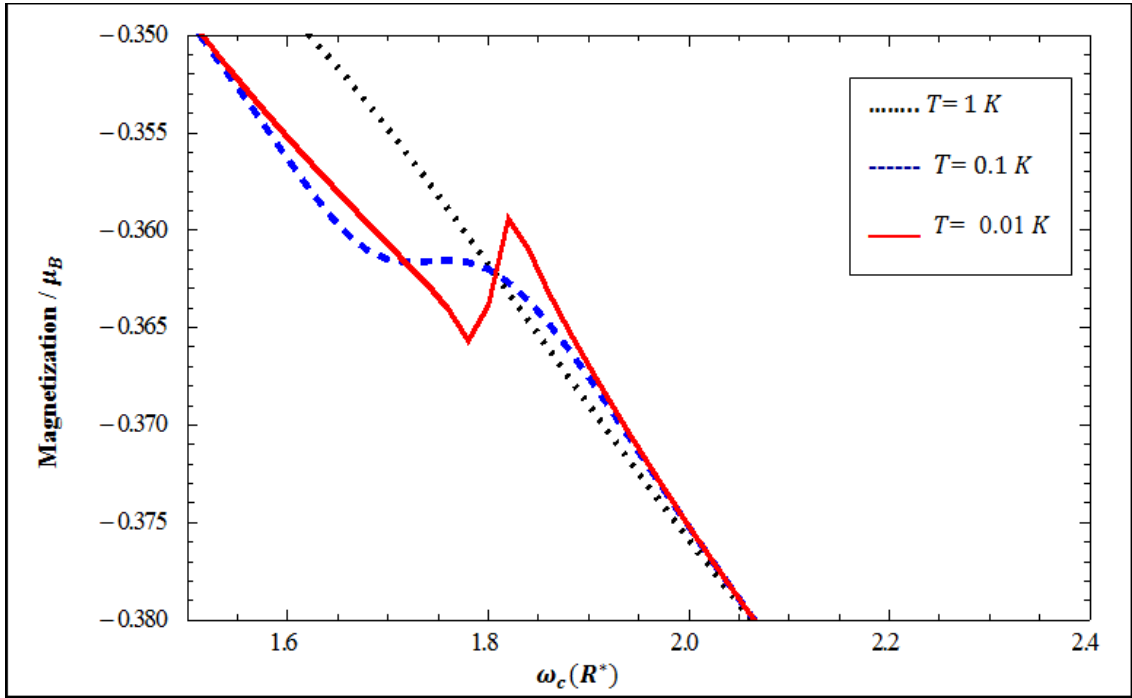


Figure (3.17): d) The magnetization (in unit of  $\mu_B = \frac{e\hbar}{2m^*} = 0.87 \text{ meV/T}$  for GaAs) of the two interacting electrons in DQD against the magnetic field strength showing the second cusp for  $\omega_o = \frac{2}{3} R^*$ ,  $\Delta = 0.5 R^*$ ,  $V_o = 1R^*$  at different temperatures. a) The (solid curve) at 0.01 K, b) the (dashed curve) at 0.1 K and c) the (dotted curve) at 1 K.

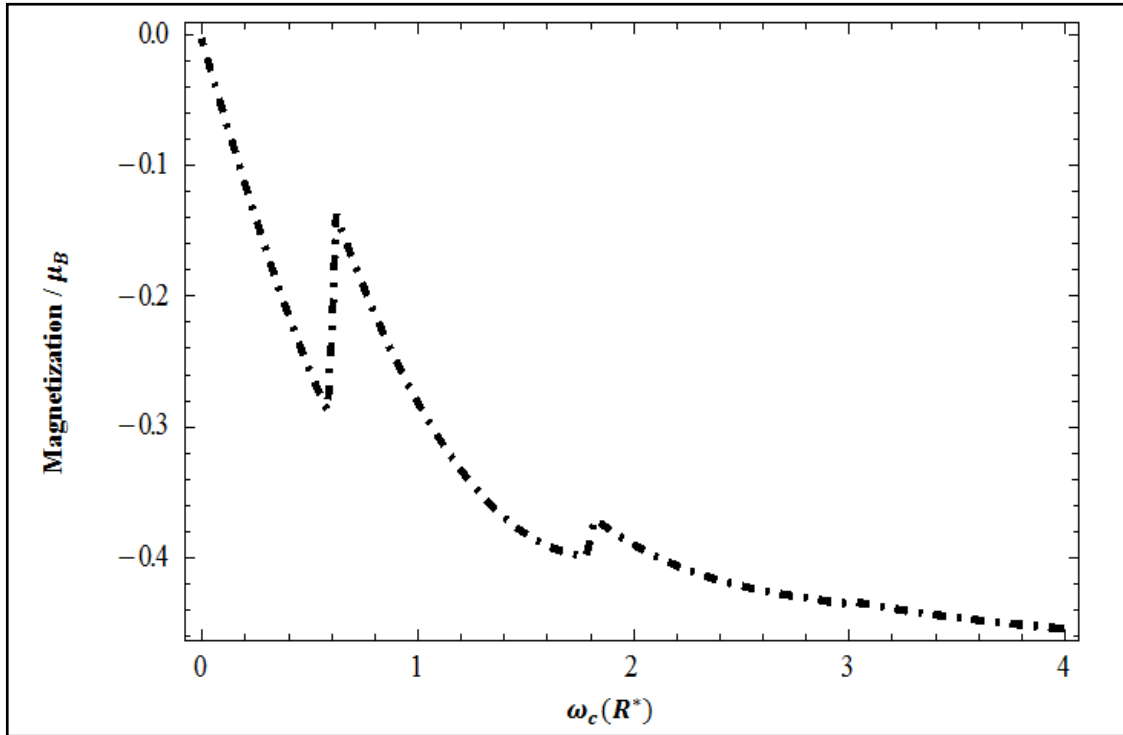


Figure (3.18):a) The magnetization (in unit of  $\mu_B \frac{e\hbar}{2m^*} 0.87 \text{ meV/T}$  for GaAs) at  $T = 0.01 \text{ K}$ , of the two interacting electrons in DQD against the magnetic field strength for  $\omega_o = \frac{2}{3} R^*$ ,  $\Delta = 0.5 R^*$  at  $V_o = 0.5 R^*$ .

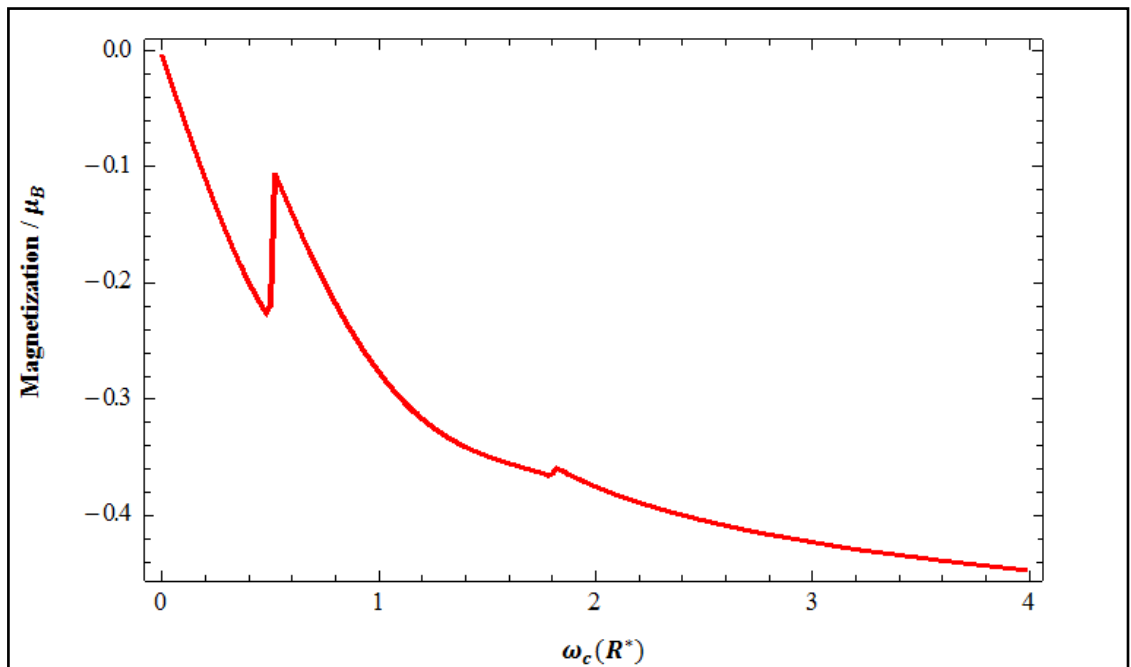


Figure (3.18): b) Same as Figure 3.18 (a) but at  $V_o = 1 R^*$ .

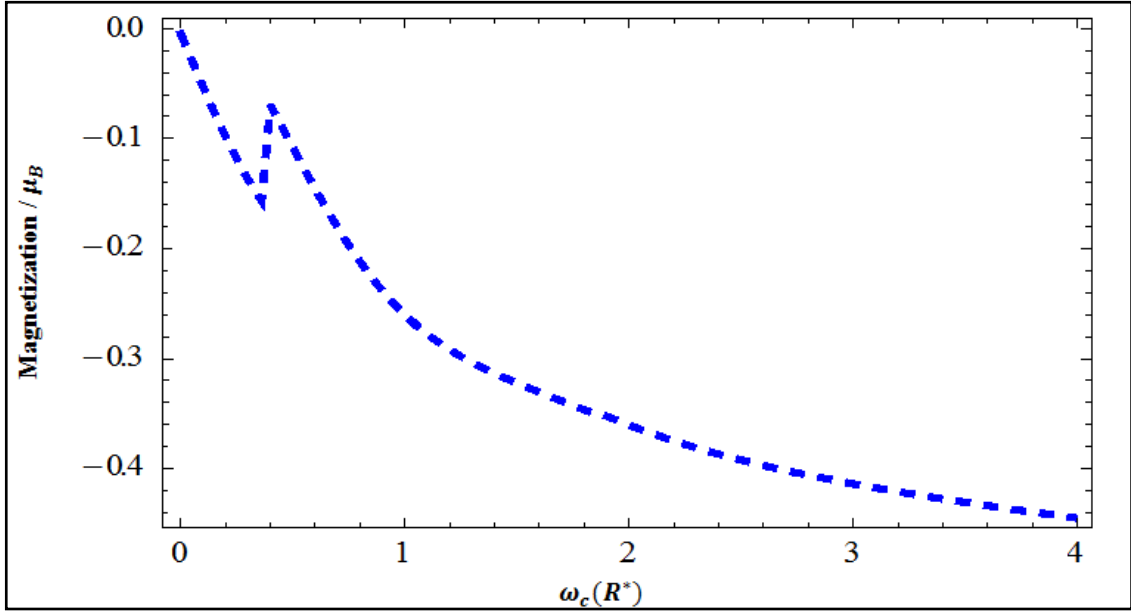


Figure (3.18): c) Same as Figure 3.18 (a) but at  $V_o = 1.5 R^*$ .

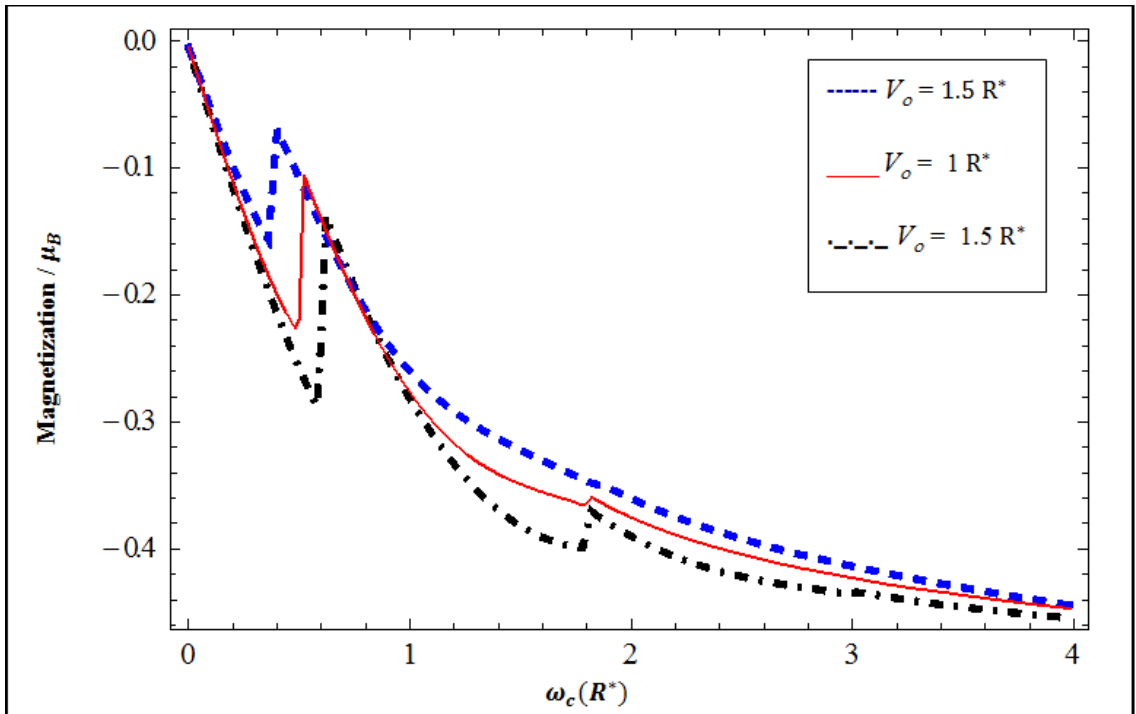


Figure (3.18): d) The magnetization (in unit of  $\mu_B = \frac{e\hbar}{2m^*} = 0.87 \text{ meV/T}$  for GaAs) at  $T = 0.01\text{K}$ , of the two interacting electrons in DQD against the magnetic field strength for  $\omega_o = \frac{2}{3} R^*$ ,  $\Delta = 0.5 R^*$  at different values of the barrier height  $V_o$ . a) The (dotted-dashed) curve at  $V_o = 0.5 R^*$ , b) the (solid) curve at  $V_o = 1R^*$  and c) at  $V_o = 1.5 R^*$ .

## Chapter Four

### Conclusion and future work

In conclusion, we had solved the Hamiltonian for two interacting electrons confined in double quantum dots under the influence of a uniform magnetic field in addition to a Gaussian barrier. The variational and the exact diagonalization techniques had been used to solve the desired Hamiltonian. Moreover, we had computed the energy spectra of the DQD system and manifested the angular momentum transitions in the ground state of double quantum dots energies which relate to (singlet-triplet) transitions. These transitions had been expressed by computing the exchange energy ( $J$ ) of the DQD system. These level transitions are caused by the coulomb interaction term in the DQD Hamiltonian. We had also deduced from our results that these transitions are the cause of the cusps in the magnetization curve of the double quantum dots system. The comparison of our results of the energy spectra and the exchange energy with other works shows a very good agreement. Furthermore, we had illustrated the dependence of the magnetization of the DQD on the parameters  $V_o$ ,  $\omega_0$ ,  $\omega_c$ ,  $\Delta$  and  $T$ .

In this work the magnetization had been studied as a thermodynamic property of the DQD system, however another thermodynamic and magnetic quantities can be taken into consideration in the future. We expect that the magnetic properties of the DQD system will be influenced appreciably by the angular momentum transitions of the ground state of the DQD energy spectra. Furthermore, the electronic and magnetic properties of few electrons DQD are serious issues to be considered in the future.

**References:**

- [1] Ashoori, R.C.; Stormer, H.L.; Weiner, J.S.; Pfeiffer, L.N.; Baldwin, K.W.; West, K. W. *Phys. Rev. Let.* **1993**, 71, 613.
- [2] Ciftja, C. *Physica Scripta* **2013**, 72, 058302.
- [3] Kastner, M.A. *Rev. Mod. Phys.* **1992**, 64, 849.
- [4] Loss, D.; Divincenzo, D.P. *Phys. Rev. A* **1998**, 57, 120.
- [5] Burkard, G.; Loss, D.; Divincenzo, D.P. *Phys. Rev. B* **1999**, 59, 2070.
- [6] Wagner, M.; Merkt, M.U.; Chaplik, A.V. *Phys. Rev. B* **1992**, 45, 1951.
- [7] Taut, M. *J. Phys. A: Math. Gen.* **1994**, 27, 1045.
- [8] Ciftja, C.; Kmar, A.A. *Phys. Rev. B* **2004**, 70, 205326.
- [9] Ciftja, O.; Golam Faruk, M. *Phys. Rev. B* **2005**, 72, 205334.
- [10] Kandemir, B.S. *Phys. Rev. B* **2005**, 72, 165350.
- [11] B.S. Kandemir, J. *Math. Phys.* **2005** 46, 032110.
- [12] Elsaid, M. *Phys. Rev. B* **2000**, 61, 13026.
- [13] Elsaid, M. *Semiconductor Sci. Technol.* **1995**, 10, 1310.
- [14] Elsaid, M. *Superlattices and Microstructures* **1998**, 23, 1237.

- [15] Elsaid, M.; Al-Naafa, M.A.; Zugail, S.J. *Comput. Theor. Nanosci.* **2008**, *5*, 677.
- [16] Elsaid, M. *Turkish J. Physics* **2002**, *26*, 331.
- [17] Maksym P.A.; Chakraborty, T. *Phys. Rev. Lett.* **1990**, *65*, 108.
- [18] De Groote, J. J. S.; Hornos, J.E.M.; Chaplik, A.V. *Phys. Rev. B* **1992**, *46*, 12773.
- [19] Nguyen, N.T.T.; Peeters, F.M. *Phys. Rev. B* **2008**, *78*, 045321.
- [20] Nammass, F.S; Sandouqa, A.S; Ghassib, H.B.; Al Sugheir, M.K. *Physica B* **2011**, *406*, 4671.
- [21] Boyacioglu, B.; Chatterjee, A. *J. Appl. Phys.* **2012**, *112*, 083514.
- [22] Helle, M.; Harju, A.; Nieminen, R.M. *Phys. Rev. B* **2005**, *72*, 205329.
- [23] Schwarz, M.P.; Grundler, D.; Wilde, M.; Heyn, Ch.; Heitmann, D. *J. Appl. Phys.* **2002**, *91*, 6875.
- [24] Räsänen, E.; Saarikoski, H.; Stavrou, V.N.; Harju, A.; Puska, M.J.; Nieminen, R.M. *Phys. Rev. B* **2003**, *67*, 235307.
- [25] Climente, J.I.; Planelles, J.; Movilla, J. L. *Phys. Rev. B* **2004**, *70*, 081301.

- [26] Avetisyan, S.; Chakraborty, T.; Pietiläinen, P. *AarXiv:1501.01025v1*  
*[cond-mat.mes-hall]*.
- [27] Fock, V. *Z. Phys.* **1928**, 47, 446.
- [28] Darwin, c.G. *Math. Proc. Cambridge Phill. Soc.* **1930**, 27, 86.
- [29] Nguyen, N.T.T.; Das Sarma, S. *Phys. Rev. B* **2011**, 83, 235322.
- [30] Dybalski, W.; Hawrylak, P. *Phys. Rev. B* **2005**, 72, 205432.

### Appendix A<sub>1</sub> : Decoupling of the single quantum dot Hamiltonian

The Hamiltonian of two interacting electron confined in single quantum dot under the effect of uniform magnetic field along z-direction is

$$H_{SQD} = \sum_{j=1}^2 \left\{ \frac{1}{2m^*} \left[ \mathbf{p}(\mathbf{r}_j) + \frac{e}{c} \mathbf{A}(\mathbf{r}_j) \right]^2 + \frac{1}{2} m^* \omega_0^2 r_j^2 \right\} + \frac{e^2}{\epsilon |\mathbf{r}_1 - \mathbf{r}_2|} \quad (A_1.1)$$

Where  $\omega_0$  is the confining frequency and  $\epsilon$  is the dielectric constant,  $\mathbf{r}_1$  and  $\mathbf{r}_2$  describe the positions of the first and second electron in the xy plane and the vector potential was taken to be

$$A(r) = \frac{1}{2} B (-y, x, 0) \quad (A_1.2)$$

$$[A, p] = 0 \quad (A_1.3)$$

$$A(r) = \frac{1}{2} B \times r \quad (A_1.4)$$

Decoupling of SQD Hamiltonian equation (2.3).

$$R = \frac{r_1 + r_2}{2} \quad (A_1.5)$$

$$r = r_2 - r_1 \quad (A_1.6)$$

$$P_R = p_1 + p_2 \quad (A_1.7)$$

$$p_r = \frac{p_2 - p_1}{2} \quad (A_1.8)$$

So the Hamiltonian can be expressed as

$$\frac{\left(\frac{eA\left[-\frac{r}{2}+R\right]}{c}-p_r+\frac{P_R}{2}\right)^2}{2m} + \frac{\left(\frac{eA\left[\frac{r}{2}+R\right]}{c}+p_r+\frac{P_R}{2}\right)^2}{2m} + \frac{1}{2}m\left(-\frac{r}{2}+R\right)^2\omega_0^2 + \frac{1}{2}m\left(\frac{r}{2}+R\right)^2\omega_0^2 + \frac{e^2}{r\epsilon} \quad (A_1.9)$$

Confining potential terms can be expressed as

$$\frac{1}{2}m\left(-\frac{r}{2}+R\right)^2\omega_0^2 + \frac{1}{2}m\left(\frac{r}{2}+R\right)^2\omega_0^2 = \frac{1}{4}mr^2\omega_0^2 + mR^2\omega_0^2 \quad (A_1.10)$$

By using the linear property of the vector potential, the kinetic energy terms can be separated into center of mass and relative part

$$\begin{aligned} & \frac{\left(\frac{eA\left[-\frac{r}{2}+R\right]}{c}-p_r+\frac{P_R}{2}\right)^2}{2m} + \frac{\left(\frac{eA\left[\frac{r}{2}+R\right]}{c}+p_r+\frac{P_R}{2}\right)^2}{2m} \\ &= \frac{\left(\frac{eA[r]}{2c}+p_r\right)^2}{m} + \frac{\left(\frac{2eA[R]}{c}+P_R\right)^2}{4m} \end{aligned} \quad (A_1.11)$$

The full single quantum dot Hamiltonian( $H_{SQD}$ ) in  $R, r$  coordinates has the following form

$$\begin{aligned} & \frac{\left(\frac{eA[r]}{2c}+p_r\right)^2}{m} + \frac{\left(\frac{2eA[R]}{c}+P_R\right)^2}{4m} + \frac{1}{4}mr^2\omega_0^2 \\ & + mR^2\omega_0^2 + \frac{e^2}{r\epsilon} \end{aligned} \quad (A_1.12)$$

The complete single quantum dot Hamiltonian  $H_{SQD}$  is separated into center of mass Hamiltonian  $H_{CM}$  and relative Hamiltonian Part  $H_r$  as shown below

$$H_{SQD} = H_{CM} + H_r \quad (A_1.13)$$

$$H_{\text{CM}} = \frac{1}{2M} \left[ P_R + \frac{Q}{c} A(R) \right]^2 + \frac{1}{2} M \omega_0^2 R^2 \quad (A_1.14)$$

$$H_r = \frac{1}{2\mu} \left[ p_r + \frac{q}{c} A(r) \right]^2 + \frac{1}{2} \mu \omega_0^2 r^2 + \frac{e^2}{\epsilon |\mathbf{r}|} \quad (A_1.15)$$

Where  $M$  is the total mass =  $2m$ ,  $Q$  is the total charge =  $2e$ ,  $\mu$  is reduce mass =  $\frac{m}{2}$ , and  $q$  is the reduced charge =  $\frac{e}{2}$ .

The center of mass part of the Hamiltonian has the well known harmonic oscillator form for the wave function and energy, this form was found Independently by Fock [27] and Darwin [28].

$$\begin{aligned} & \psi_{n_2, m_2}(R) \\ &= (-1)^{n_2} \frac{\beta^{|m_2+1|}}{\sqrt{\pi}} \left[ \frac{n_2!}{(n_2 + |m_2|)!} \right]^{\frac{1}{2}} e^{-\beta^2 R^2 / 2} R^{|m_2|} L_{n_2}^{|m_2|} \beta^2 R^2 e^{im_2 \phi} \end{aligned} \quad (A_1.16)$$

$$E_{n_{\text{cm}}, m_{\text{cm}}} = (2n_{\text{cm}} + |m_{\text{cm}}| + 1) \hbar \sqrt{\frac{\omega_c^2}{4} + \omega_0^2} + m_{\text{cm}} \frac{\hbar \omega_c}{2} \quad (A_1.17)$$

Where  $n_{\text{cm}}, m_{\text{cm}}$  are the radial and azimuthal quantum numbers, respectively. And  $L_n^m$  is the associate laguerre polynomial.

The relative Hamiltonian part does not have analytic solution so it had been solved variationally.

By the help of a symmetric gauge, the relative Hamiltonian part can be written as :

$$\begin{aligned} H_r = \frac{1}{2\mu} \left( p_r^2 + \frac{q^2}{c^2} \frac{1}{4} B^2 r^2 + (-1) \frac{q}{c} \vec{L} \cdot \vec{B} \right) + \frac{1}{2} \mu \omega_0^2 r^2 \\ + \frac{e^2}{\epsilon |\mathbf{r}|} \end{aligned} \quad (A_1.18)$$

Where the magnetic field is uniform with strength  $\omega_c = \frac{eB}{cm}$  and taken to be along z direction.

$$\vec{L} \cdot \vec{B} = L_z B \quad (A_1.19)$$

$$\begin{aligned} \frac{p_r^2}{m} + \frac{1}{16} \omega_c m r^2 + \frac{1}{2} \omega_c L_z + \frac{1}{4} m \omega_0^2 r^2 + \frac{e^2}{\epsilon |\mathbf{r}|} \\ = \frac{p_r^2}{m} + \frac{1}{4} m r^2 \left( \frac{\omega_c^2}{4} + \omega_0^2 \right) + \frac{1}{2} \omega_c L_z + \frac{e^2}{\epsilon |\mathbf{r}|} \end{aligned} \quad (A_1.20)$$

## Appendix A<sub>2</sub>: Variation of parameter method of the SQD Hamiltonian

The main idea for variational method that choosing the variational wave function with parameters  $\varepsilon_i$

$$\Psi = \psi(\varepsilon_1, \varepsilon_2, \dots, \varepsilon_j) \quad (A_{2.1})$$

and obtain the energy by solving Schrödinger equation

$$H \Psi = E \Psi \quad (A_{2.2})$$

To get the energy in terms of the variational parameter, we have to minimize the energy formula  $E(\varepsilon_1, \varepsilon_2, \dots, \varepsilon_j)$  with respect to each variational parameter  $\varepsilon_i$  to get a stable system

$$\frac{\partial E \left( (\varepsilon_1, \varepsilon_2, \dots, \varepsilon_j) \right)}{\partial \varepsilon_i} = 0 \quad (A_{2.3})$$

$$\frac{\partial^2 E \left( (\varepsilon_1, \varepsilon_2, \dots, \varepsilon_j) \right)}{\partial \varepsilon_i^2} > 0 \quad (A_{2.4})$$

For  $i = 1, 2, \dots$

The adopted one parameter variational wave function is :

$$\psi(r) = \sqrt[4]{\alpha} \frac{u_m(\rho) e^{im\phi}}{\sqrt{2\pi} \sqrt{\rho}} \quad (A_{2.5})$$

Where,

$$u_m(\rho) = \rho^{1/2+|m|} (1 + \beta\rho) e^{-\left(\frac{\rho^2}{2}\right)} \quad (A_{2.6})$$

$$\rho = \sqrt{\alpha} r \quad (A_2.7)$$

In our calculations, we have used the following Atomic Rydberg units

$$e^2 = 2, \hbar = 1, m = 1, \epsilon = 1 \quad (A_2.8)$$

The normalization constant of the variational wave function (equation 2.8) is defined as follows

$$C_m^2 = \frac{\sqrt{\alpha}}{d + e\beta + f\beta^2} \quad (A_2.9)$$

Where,

$$d = \frac{1}{2 \Gamma[1 + |m|]} \quad (A_2.10)$$

$$e = \Gamma\left[\frac{3}{2} + |m|\right] \quad (A_2.11)$$

$$f = \frac{1}{2\Gamma[2 + |m|]} \quad (A_2.12)$$

The energies of the relative part of  $H_{SQD}$  is given in terms of the variational parameter as follows :

$$E_r(\beta) = -\frac{1}{2}m\omega_c + 2\alpha \frac{a + b\beta + c\beta^2}{d + e\beta + f\beta^2} \quad (A_2.13)$$

Where a, b and c are constants in terms of quantum numbers m and  $\alpha$ , given explicitly as follows :

$$a = \frac{e}{(2|m| + 1)\sqrt{\alpha}} + 2f \quad (A_2.14)$$

$$b = \frac{2d}{\sqrt{\alpha}} + 2(|m| + 1)e \quad (A_2.15)$$

$$c = \frac{e}{2\sqrt{\alpha}} + (2|m|^2 + 4|m| + 3)d \quad (A_2.16)$$

d, e, f which is previously defined in Equation (A<sub>2</sub>.10 - A<sub>2</sub>.12) respectively.

The value of the parameter  $\beta$  which satisfies the minimum energy requirement is

$$\beta_{min,m} = \frac{2cd - 2af - \sqrt{(2cd - 2af)^2 - 4(bd - ae)(ce - bf)}}{2(-ce + bf)} \quad (A_2.17)$$

So, the energy expression of the SQD Hamiltonian in terms of the variational parameter value which satisfies the minimization condition is :

$$E_r(\beta_{min}) = -\frac{1}{2}m\omega_c + 2\alpha \frac{a+b\beta_{min}+c\beta_{min}^2}{d+e\beta_{min}+f\beta_{min}^2} \quad (A_2.18)$$

### Appendix A<sub>3</sub>: The exact diagonalization technique

Consider the eigenvalue formula:

$$\hat{H} |\psi \rangle = E |\psi \rangle \quad (A_3.1)$$

$$|\psi \rangle = \sum_n |\varphi_n \rangle \quad (A_3.2)$$

$$\hat{H} \sum_n |\varphi_n \rangle = E_n \sum_n |\varphi_n \rangle \quad (A_3.3)$$

Multiply Eqn (A<sub>3</sub>.3) by  $\langle \varphi_m |$  from both sides

$$\sum_n \langle \varphi_m | H | \varphi_n \rangle = E_n \sum_n \langle \varphi_m | \varphi_n \rangle \quad (A_3.4)$$

$$\text{But } \sum_n \langle \varphi_m | H | \varphi_n \rangle = \sum_n H_{mn} \quad (A_3.5)$$

Then Eqn (A<sub>3</sub>.4) becomes

$$\sum_n H_{mn} = E_n \sum_n \langle \varphi_m | \varphi_n \rangle \quad (A_3.6)$$

$$\sum_n \langle \varphi_m | \varphi_n \rangle = \delta_{mn} \quad (A_3.7)$$

$$\sum_n [H_{mn} - E_n \delta_{mn}] = 0 \quad (A_3.8)$$

Then the secular characteristic equation is

$$\text{Det} [H_{mn} - E_n \delta_{mn}] = 0 \quad (A_3.9)$$

جامعة النجاح الوطنية

كلية الدراسات العليا

# التمغظ لزوج من النقاط الكمية (GaAs) في مجال مغناطيسي

إعداد

اشتياق "محمد ياسر" حجاز

إشراف

أ. د. محمد السعيد

د. موسى الحسن

قدمت هذه الأطروحة استكمالاً لمتطلبات الحصول على درجة الماجستير في الفيزياء  
في كلية الدراسات العليا في جامعة النجاح الوطنية - نابلس.

2016

ب

التمغنت لزوج من النقاط الكمية

(GaAs) في مجال مغناطيسي

إعداد

اشتياق "محمد ياسر" حجاز

إشراف

أ.د. محمد السعيد

د. موسى الحسن

المخلص

تم حساب التمغنت لزوج من الإلكترونات المتشادة والمحصورة في زوج من النقاط الكمية تحت تأثير مجال مغناطيسي في الاتجاه الزيني بالإضافة إلى حاجز غاوسي وذلك عن طريق حل دالة هاملتون باستخدام طريقة المتغيرات وطريقة القطر الدقيقة. ولقد قمنا أيضا بدراسة اعتماد التمغنت على كل من درجة الحرارة والمجال المغناطيسي وتردد الحصر بالإضافة إلى ارتفاع الحاجز وعرضه. كما وضحت الدراسة الانتقال الأحادي-الثلاثي للزخم الزاوي للمستوى الأرضي لزوج من النقاط الكمية والقفزات في منحنى التمغنت الناتجة عنه. وأظهرت المقارنات توافق كبير بين نتائجنا مع نتائج أعمال أخرى منشورة.